

Linear, Mixed-Valent Homocatenated Tri-Tin Complexes Featuring Sn-Sn Bonds

Wei-Chieh Chang, Anki Raj, Hirotugu Hiramatsu, Han-Jung Li, Micah S. Ziegler, Yichen Lin,
ShengCih Huang and Hsueh-Ju Liu*

Table of Contents

Page S2	1. Experimental details, synthetic procedures, characterizations	
Page S14	2. Details on Raman measurement and data analysis	
Page S15	3. Single-crystal X-ray diffraction crystal structure figures and data tables	
Page S28	4. Computational details	
Page S32	5.	References

1. Experimental details, synthetic procedures, and characterizations

All manipulations with oxygen and moisture sensitive materials were performed in a nitrogen-filled glovebox. Solvents were dried and deaerated using a solvent system (AsiaWong Enterprise co., Ltd.) prior to use. Acetonitrile- d_3 (MeCN- d_3) was dried over CaH₂ and degassed by three freeze-pump-thaw cycles and stored under nitrogen over 3 Å molecular sieves. Benzene- d_6 and tetrahydrofuran- d_8 (THF- d_8) was dried over sodium and benzophenone, degassed by three freeze-pump-thaw cycles, and stored under nitrogen over 3 Å molecular sieves. The compounds L^{Ph}H,^[1] Sn(HMDS)₂^[2] and Sn(HMDS)Cl^[2a] were prepared according to literature procedures. The NMR spectra were recorded using Bruker 300, Varian 400 or Varian 600 MHz spectrometers. The NMR spectra were referenced to residual protonated solvent for ¹H NMR (3.58 ppm for compound in THF- d_8 or THF- d_8 /MeCN- d_3 (1:1) co-solvent), to deuterated solvent for ¹³C NMR (67.21 ppm for compound in THF- d_8 or THF- d_8 /MeCN- d_3 (1:1) co-solvent), and to tetra-*n*-butyltin for ¹¹⁹Sn NMR (−11.7 ppm in THF- d_8). All spectra were recorded at 25°C. Complex multiplets are noted as “m” and broad resonances as “br”.

Elemental analyses were performed using an Elementar vario EL CUBE (CHN-OS Rapid, German).

Mass spectra of the (L^{Ph}Sn)₃Cl solutions were acquired by direct infusion (2 μL). ESI(+)-MS experiments were carried out using an Impact HD Q-TOF mass spectrometer (Bruker, Germany) equipped with an electrospray ionization (ESI) source operating in positive ion mode. The parameters of ESI(+) included 4.5 kV for ion spray voltage, 200 °C for capillary temperature, and 6 L/min for sheath gas flow rate. The mass spectra were collected over the mass range of *m/z* 500-3000 at a resolving power of 40000. The collected data were analyzed using Compass DataAnalysis 4.1 (Bruker, Germany).

UV-visible spectra were recorded using Hitachi U-3010 Spectrophotometer equipped with a diffuse reflectance sample stage.

Synthesis of L^{Ph}SnCl.

A solution of L^{Ph}H (3.153 g, 8.44 mmol) in 30 mL of THF was added to a solution of Sn(HMDS)Cl (2.656 g, 8.44 mmol) in 30 mL of THF at ambient temperature. The yellow solid formed in 10 min. After stirring at ambient temperature for 3 h, the mixture was cooled to −35 °C, and the supernatant was removed by decanting. The remaining solid was washed three times with 10 mL of pentane and then dried under vacuum to afford a yellow powder. Yield: 4.256 g (96%). Light yellow-green crystals were obtained by diffusion of pentane into a saturated THF solution of L^{Ph}SnCl at ambient temperature for a few days. ¹H NMR (599.63 MHz, THF- d_8) δ 8.54 (d, *J* = 4.8 Hz, 2H), 7.55 (d, *J* = 7.8 Hz, 2H), 7.32–7.18 (m, 10H), 7.17–7.10 (m, 4H) ppm; ¹³C{¹H} NMR (150.81 MHz, THF- d_8) δ = 151.67, 147.07, 139.22, 137.03, 134.61, 131.54, 130.27, 128.73, 127.25, 121.39, 119.92 ppm; ¹¹⁹Sn{¹H} NMR (224.85 MHz, THF- d_8): −416.43 ppm. Anal. calcd for C₂₆H₁₈N₃SnCl: C, 59.30; H, 3.45; N, 7.98. Found: C, 59.46; H, 3.45; N, 8.19.

Synthesis of (L^{Ph}Sn)₃Cl.

To a solution of L^{Ph}SnCl (0.103 g, 0.195 mmol) in THF (10 mL), LiB^sBu₃H (L-Selectride, 0.13 mL of a 1M solution in THF (AcroSeal®, Acros), 0.130 mmol, 0.66 equiv.) was added dropwise at ambient temperature. Within a few minutes, the reaction mixture turned from light yellow green to dark red. The reaction mixture was stirred at ambient temperature for 7 h. Then, all volatile materials were removed *in vacuo*. After washing the resulting solid with 5 mL of pentane, the residue was extracted with toluene (30 mL), and the resulting mixture filtered through a plug of Celite. The filtrate was concentrated and residual volatile compounds were removed *in vacuo*, and the resulting solid was re-dissolved in THF. Pentane (10 mL) was layered over the THF solution and allowed to stand for 2 days at −35 °C, affording analytically pure dark red crystals. Yield: 0.062 (55%). ¹H NMR (300.13 MHz, THF- d_8 and MeCN- d_3 (1:1)) δ = 8.26 (br, 6H), 7.45 (t, *J* = 7.8 Hz, 6H), 7.30–7.16 (m, 18H), 7.14–6.85 (m, 24H) ppm; ¹³C{¹H} NMR (75.47 MHz, THF- d_8 and MeCN- d_3 (1:1)) δ = 147.01, 131.52, 128.80 ppm; ¹¹⁹Sn{¹H} NMR (224.85 MHz, THF- d_8): −113.6, −415.23 ppm. UV-vis: 543, 671 in solid state, 0.87 % w/w with NaCl_(s); 676 (ε =

8674) in THF; 513 ($\epsilon = 11327$), 645 ($\epsilon = 3572$) in MeCN, Anal. calcd for $C_{82}H_{62}ON_9Sn_3Cl$ [$(L^{Ph}Sn)_3Cl \cdot THF$]: C, 62.29; H, 3.95; N, 7.97. Found: C, 62.58; H, 4.29; N, 7.72.

Synthesis of $(L^{Ph})_2Sn$.

Treatment of a solution of $L^{Ph}H$ (1.549 g, 4.15 mmol) in 30 mL toluene with $Sn(HMDS)_2$ (0.911 g, 2.07 mmol) gave a mixture with yellow precipitate after stirring at ambient temperature for 16 hr. The resulting precipitate was washed with pentane and $(L^{Ph})_2Sn$ was obtained as a yellow solid. Yield: 1.765 g (98%). Analytically pure $(L^{Ph})_2Sn$ was recrystallized by slow evaporation of a saturated THF solution at ambient temperature. 1H NMR (399.77 MHz, THF- d_8) $\delta = 8.43$ (d, $J = 5.2$ Hz, 2H), 7.40-7.03 (m, 14H), 6.78 (d, $J = 6.3$ Hz, 2H) ppm. Due to the low solubility of $(L^{Ph})_2Sn$ in benzene- d_6 , THF- d_8 or 1:1 THF- d_8 /MeCN- d_3 (<1-2 mg/mL), only very weak ^{13}C resonances were observed after many scans and thus they are not reported. Anal. calcd for $C_{52}H_{36}N_6Sn$: C, 72.32; H, 4.20; N, 9.73. Found: C, 72.29; H, 4.04; N, 9.56.

Synthesis of $(L^{Ph}Sn)_3OTf$.

A solution of $(L^{Ph}Sn)_3Cl$ (0.075 g, 0.044 mmol) in 8 mL of THF/MeCN (1:1) was added to NaOTf (0.008 g, 0.044 mmol) at ambient temperature. Upon stirring for 5 min, the reaction mixture was filtered through a plug of Celite. The filtrate was layered with 10 mL of pentane at $-35^\circ C$ to afford analytically pure red crystals. Yield: 0.061 g (87%). 1H NMR (300.13 MHz, THF- d_8 /MeCN- d_3 (1:1)) $\delta = 7.81$ (d, $J = 5.1$ Hz, 6H), 7.50 (t, $J = 7.8$ Hz, 6H), 7.29 – 7.16 (m, 18H), 7.07 – 6.80 (m, 24H) ppm; $^{13}C\{^1H\}$ NMR (75.47 MHz, THF- d_8 /MeCN- d_3 (1:1)) $\delta = 151.04, 146.29, 138.70, 136.35, 132.64, 131.47, 129.99, 128.71, 127.41, 120.66, 120.06$ ppm. Due to the low solubility of $(L^{Ph}Sn)_3OTf$ in THF- d_8 or THF- d_8 /MeCN- d_3 mixed solvent (<1-2 mg/mL), no ^{119}Sn resonances were observed even after many scans. UV-vis: 516 ($\epsilon = 16422$) in THF. Anal. calcd for $C_{79}H_{54}N_9SO_3F_3Sn_3$: C, 58.48; H, 3.35; N, 7.77. Found: C, 58.57; H, 3.58; N, 7.99. HR-ESIMS calcd for $C_{79}H_{58}N_9OSn_3^+$ ($(L^{Ph}Sn)_3 \cdot MeOH$) $^+$: 1508.1825. Found: 1508.1536.

Synthesis of $(L^{Ph}Sn)_3PF_6$.

A solution of $(L^{Ph}Sn)_3Cl$ (0.061 g, 0.036 mmol) in 6 mL of THF/MeCN (1:1) was added to KPF_6 (0.007 g, 0.036 mmol) at ambient temperature. Upon stirring for 5 min, the reaction mixture was filtered through a plug of Celite. The filtrate was layered with 12 mL of diethyl ether at $-35^\circ C$ to afford analytically pure red crystals. Yield: 0.035 g (61%). 1H NMR (300.13 MHz, THF- d_8 /MeCN- d_3 (1:1)) $\delta = 7.81$ (d, $J = 4.9$ Hz, 6H), 7.50 (t, $J = 7.8$ Hz, 6H), 7.30 – 7.16 (m, 18H), 7.14 – 6.85 (m, 24H) ppm; $^{13}C\{^1H\}$ NMR (75.47 MHz, THF- d_8 /MeCN- d_3 (1:1)) $\delta = 151.04, 146.28, 138.72, 136.34, 132.64, 131.46, 130.00, 128.71, 127.42, 120.67, 120.06$ ppm. Due to the low solubility of $(L^{Ph}Sn)_3PF_6$ in THF- d_8 or THF- d_8 /MeCN- d_3 mixed solvent (<1-2 mg/mL), no ^{119}Sn resonances were found after prolonged scans. UV-vis: 516 ($\epsilon = 17368$), 668 ($\epsilon = 2249$) in THF. Anal. calcd for $C_{78}H_{54}N_9Sn_3PF_6$: C, 57.89; H, 3.36; N, 7.79. Found: C, 57.68; H, 3.39; N, 7.65.

Synthesis of $(L^{Ph}Sn)_3AlCl_4$.

A solution of $(L^{Ph}Sn)_3Cl$ (0.0469 g, 0.0311 mmol) in 6 mL of THF was added to $AlCl_3$ (0.0042 g, 0.031 mmol) at ambient temperature. Upon stirring for 5 min, the reaction mixture was filtered over celite. The filtrate was layered with 10 mL of Et_2O at $-35^\circ C$ to afford an nearly analytically pure red solid. Yield: 0.0317 g (62%). 1H NMR (300 MHz, THF- d_8 and MeCN- d_3 (1:1), $25^\circ C$) $\delta = 7.85$ (d, $J = 4.8$ Hz, 6H), 7.51 (t, $J = 7.8$ Hz, 6H), 7.28 – 7.16 (m, 18H), 7.01 – 6.86 (m, 24H) ppm; $^{13}C\{^1H\}$ NMR (75 MHz, THF- d_8 and MeCN- d_3 (1:1), $25^\circ C$) $\delta = 151.09, 146.40, 138.90, 136.33, 132.82, 131.45, 130.06, 128.74, 127.45, 120.85, 120.06$ ppm. Due to the low solubility of $(L^{Ph}Sn)_3PF_6$ in THF- d_8 or THF- d_8 /MeCN- d_3 mixed solvent (<1-2 mg/mL), no ^{119}Sn resonances were found after prolonged scans. Anal. calcd for $C_{78}H_{54}N_9AlCl_4Sn_3$: C, 57.05; H, 3.31; N, 7.68. Found: C, 56.50; H, 3.21; N, 7.55.

Synthesis of $(L^{Ph}Sn)_2(W(CO)_5)_2$.

A 4mL THF solution of $W(CO)_6$ (0.0045g, 0.013 mmol) was irradiated under UV light (254 nm, 16 hr). The resulting solution was added to a solution of $(L^{Ph}Sn)_3Cl$ (0.0469 g, 0.0311 mmol) in 2 mL of THF at ambient temperature. After stirring for 2 hours, the solution was layered with pentane to afford

characterizable yellow crystals. Yield: 76%. **¹H NMR** (600 MHz, C₆D₆, 25 °C) δ = 8.38 (d, *J* = 4.8 Hz, 4H), 7.26 – 7.0 (m, 24H), 6.66 (t, *J* = 7.8 Hz, 4H) 6.49 (t, *J* = 6.3 Hz, 4H) ppm; **¹³C{¹H} NMR** (75 MHz, C₆D₆, 25 °C) δ = 201.77, 200.01, 150.01, 145.84, 138.61, 135.70, 132.11, 131.11, 130.65, 127.82, 127.36, 121.11, 119.97 ppm; **¹¹⁹Sn{¹H} NMR** (223 MHz, C₆D₆): –94.96 ppm. Anal. calcd for C₆₂H₃₆N₆O₁₀Sn₂W₂: C, 45.68; H, 2.23; N, 5.16. Found: C, 45.90; H, 2.37; N, 5.11.

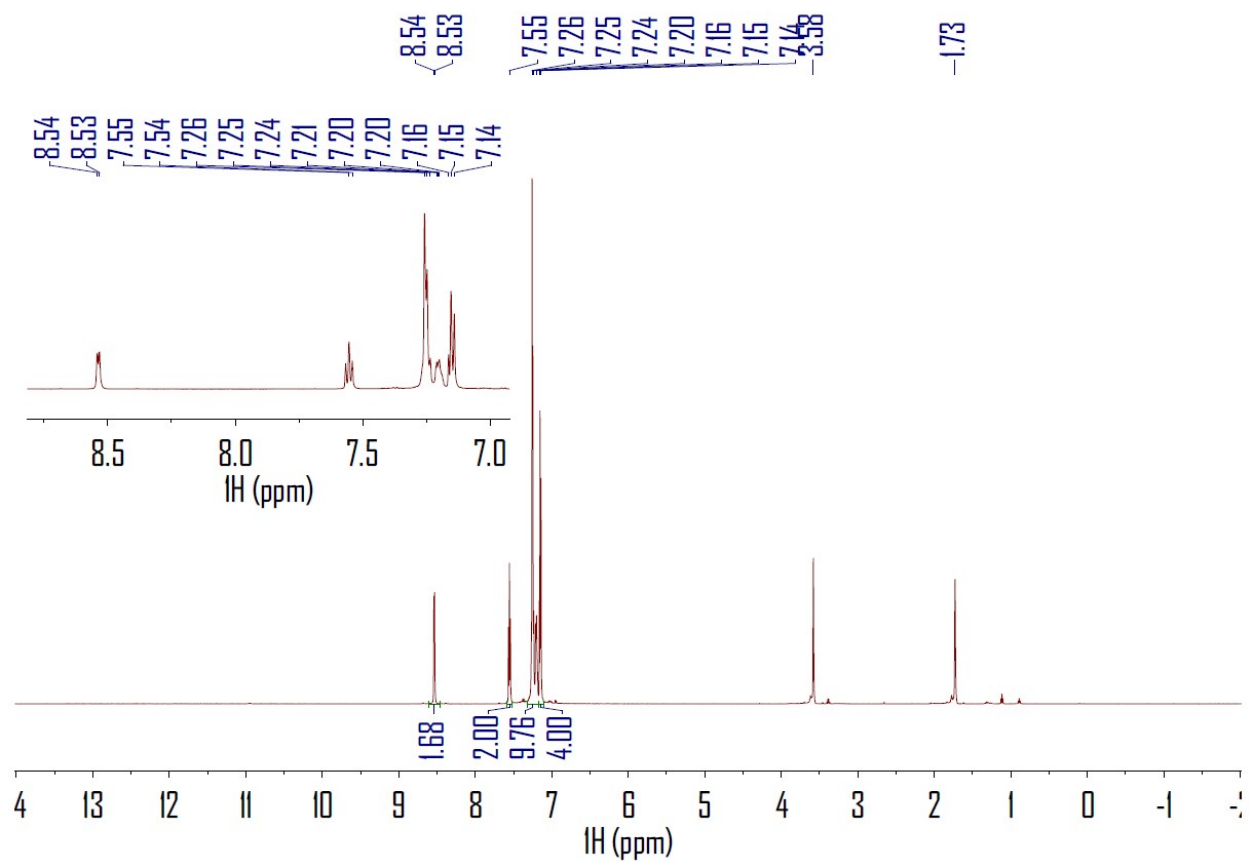


Figure S1. ^1H NMR spectrum of $\text{L}^{\text{Ph}}\text{SnCl}$ in $\text{THF-}d_8$.

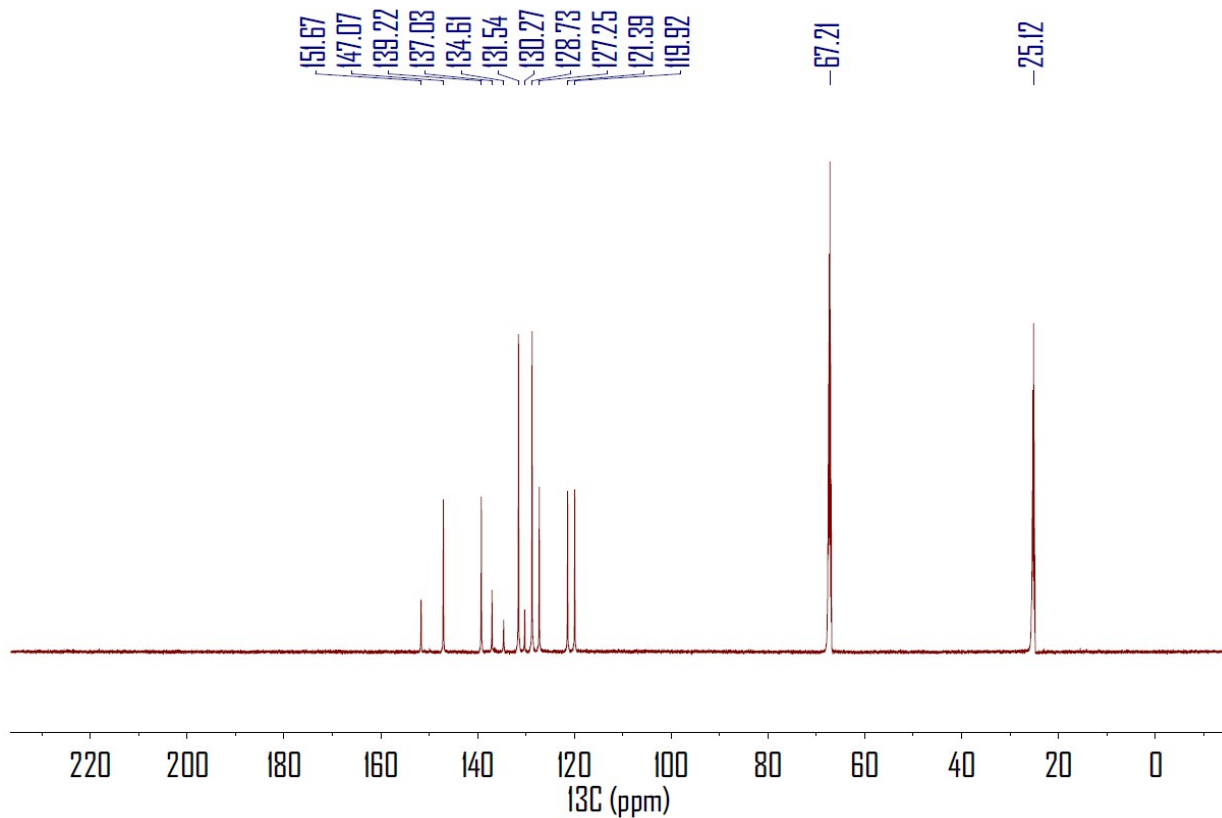


Figure S2. $^{13}\text{C}\{^1\text{H}\}$ NMR spectrum of $\text{L}^{\text{Ph}}\text{SnCl}$ in $\text{THF-}d_8$.

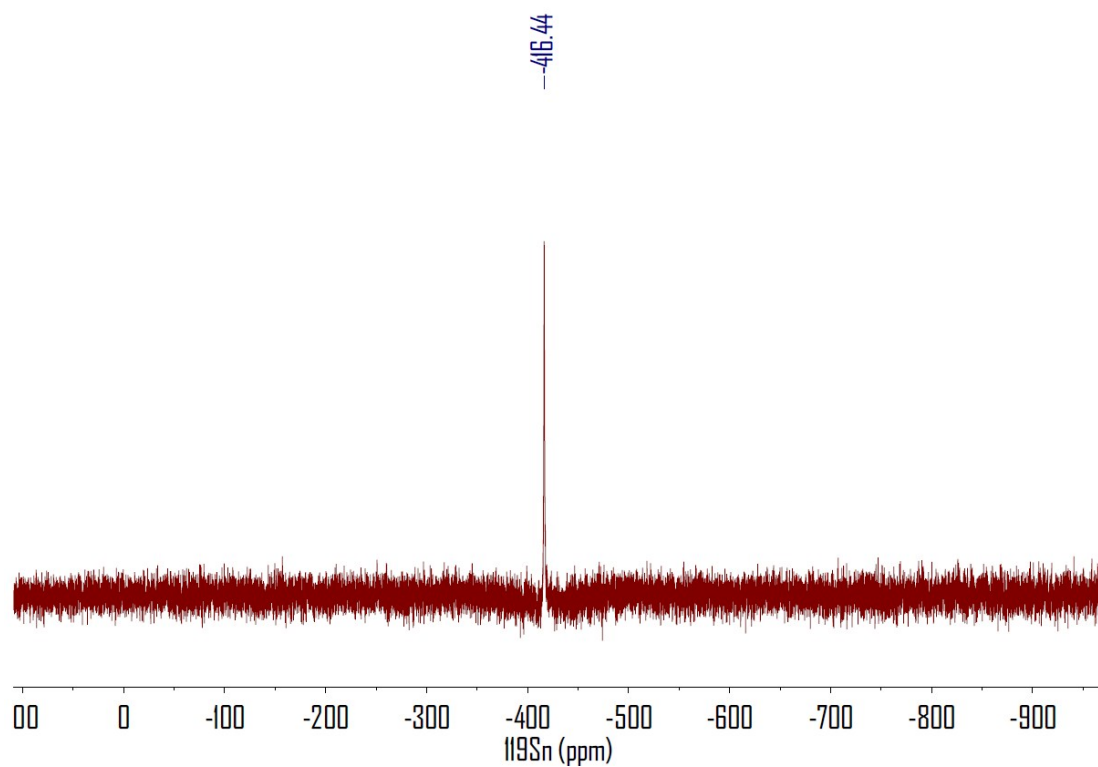


Figure S3. $^{119}\text{Sn}\{^1\text{H}\}$ NMR spectrum of $\text{L}^{\text{Ph}}\text{SnCl}$ in $\text{THF-}d_8$.

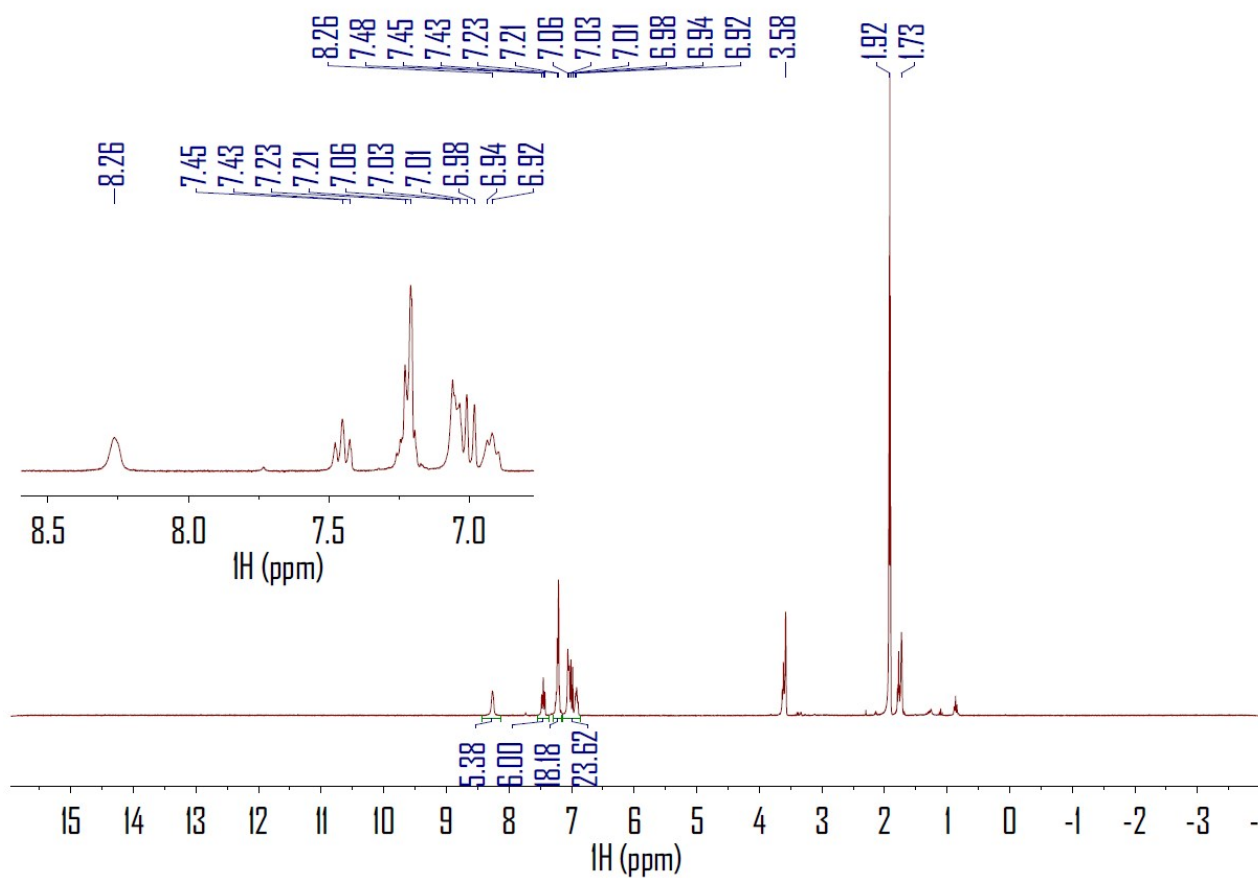


Figure S4. ^1H NMR spectrum of $(\text{L}^{\text{Ph}}\text{Sn})_3\text{Cl}$ in $\text{THF-}d_8/\text{MeCN-}d_3$ (1:1).

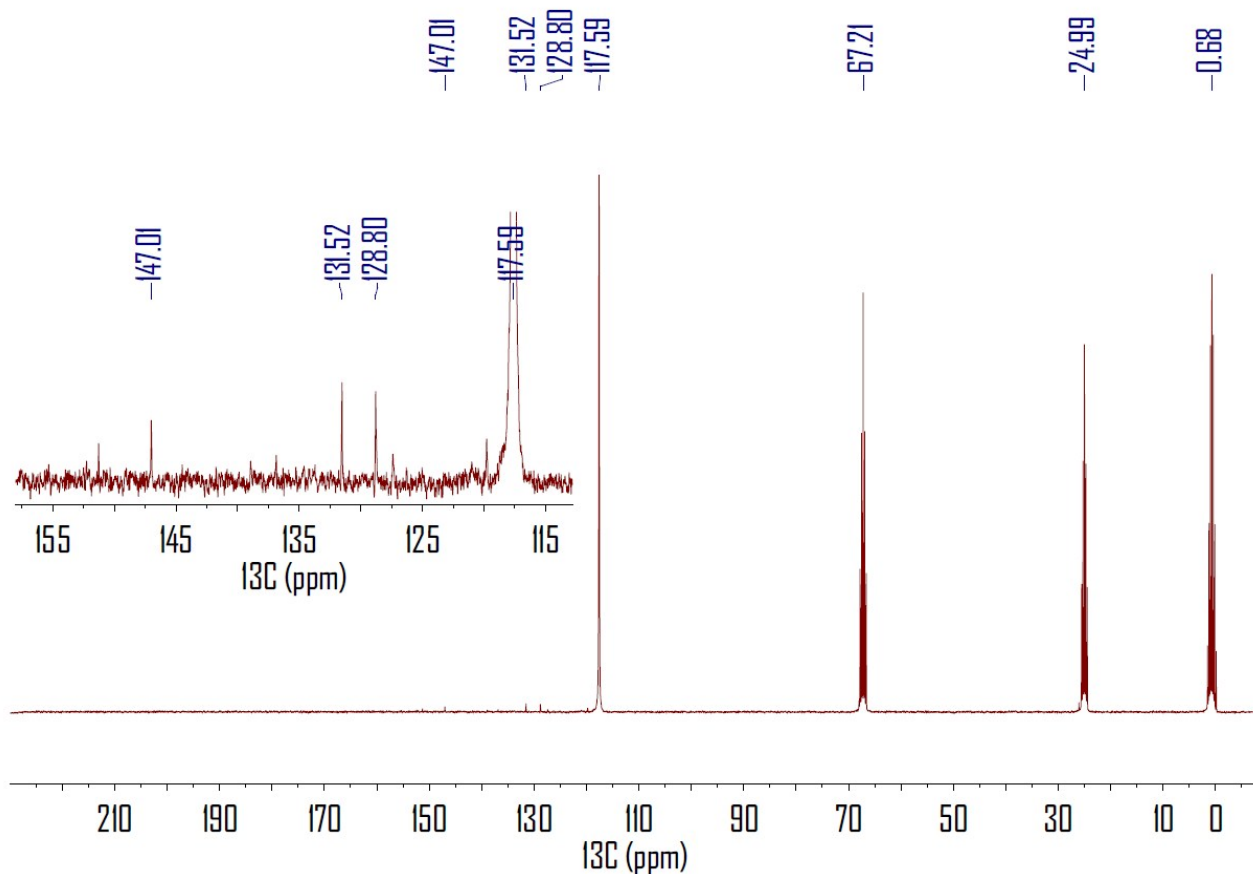


Figure S5. $^{13}\text{C}\{^1\text{H}\}$ NMR spectrum of $(\text{L}^{\text{Ph}}\text{Sn})_3\text{Cl}$ in $\text{THF-}d_8/\text{MeCN-}d_3$ (1:1).

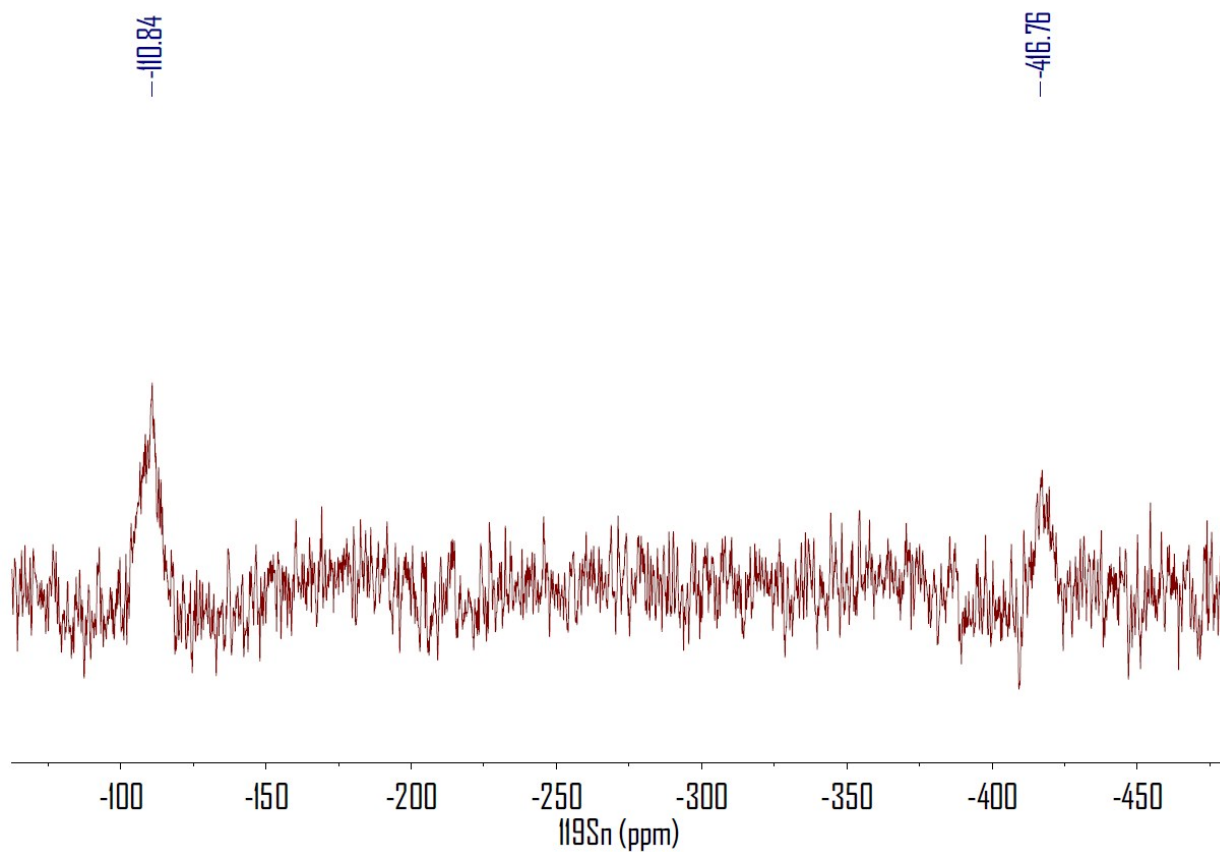
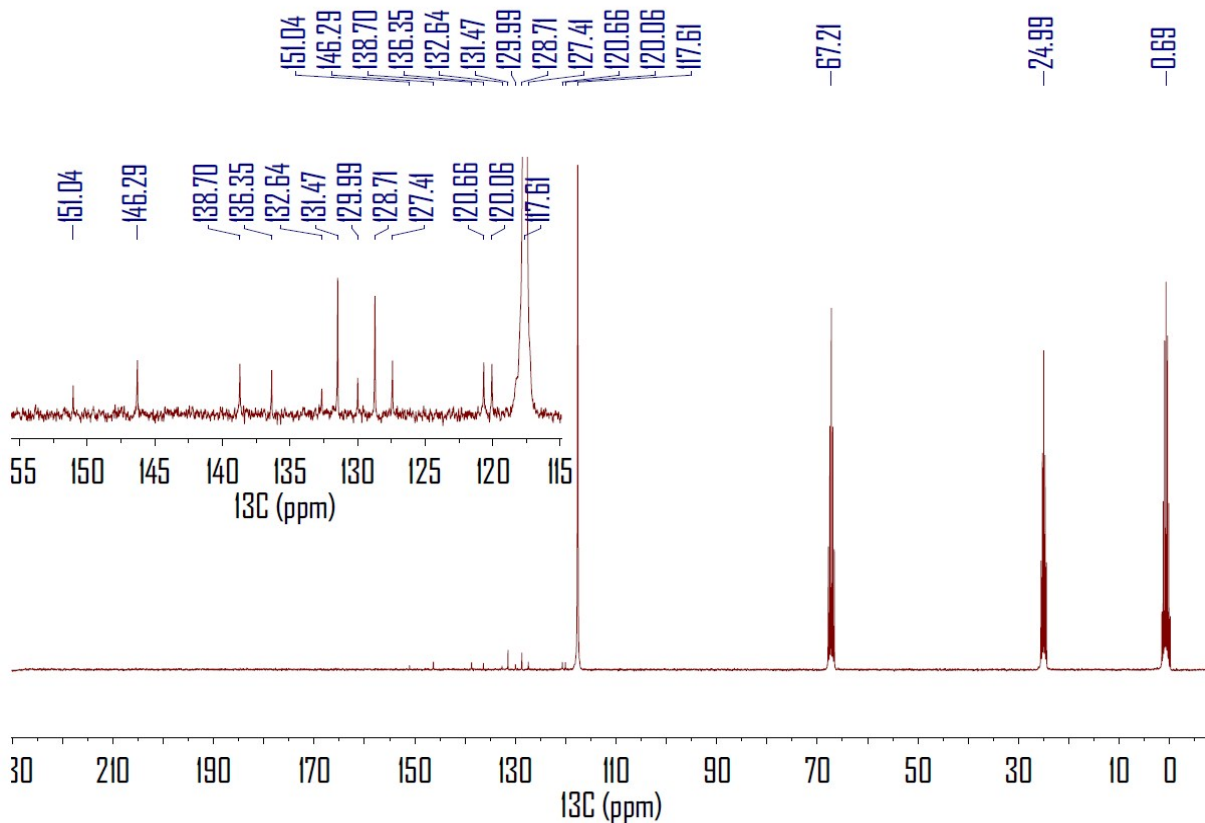
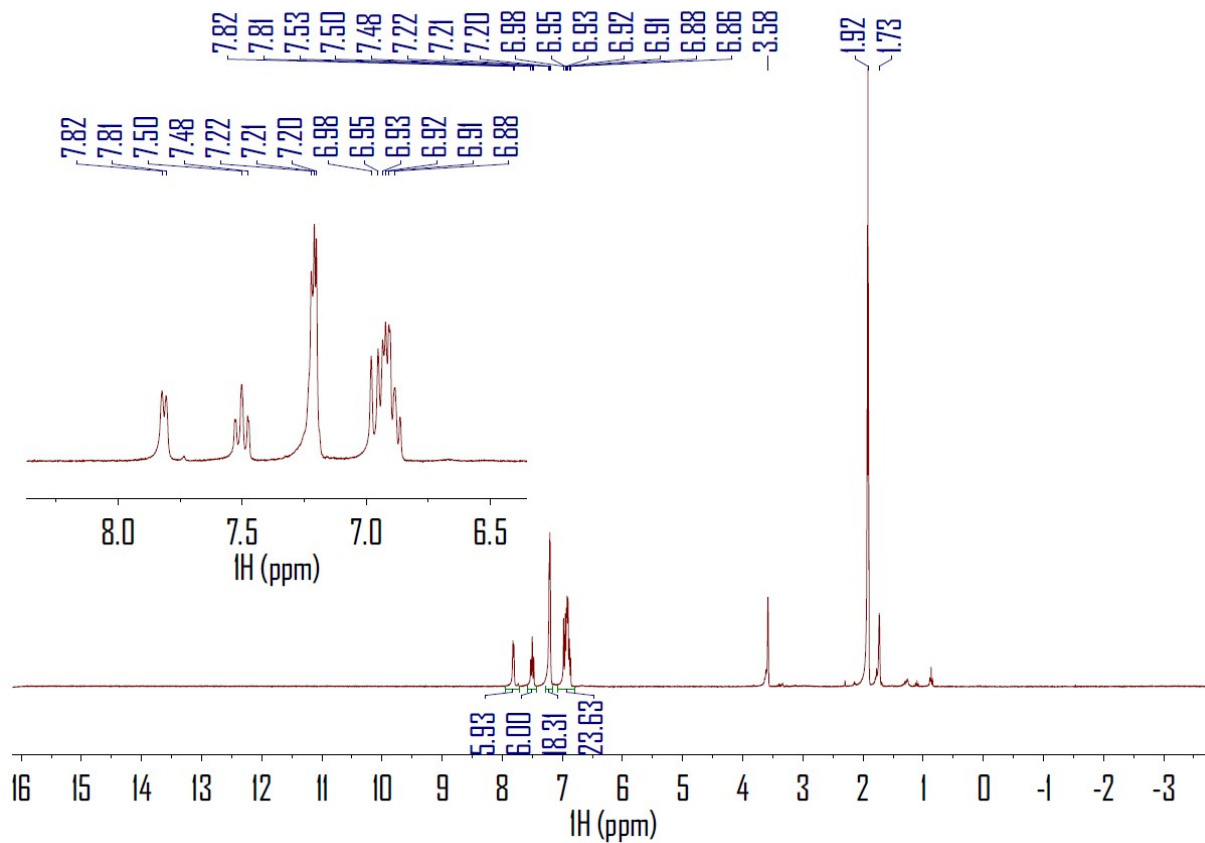


Figure S6. $^{119}\text{Sn}\{^1\text{H}\}$ NMR spectrum of $(\text{L}^{\text{Ph}}\text{Sn})_3\text{Cl}$ in $\text{THF-}d_8/\text{MeCN-}d_3$ (1:1).



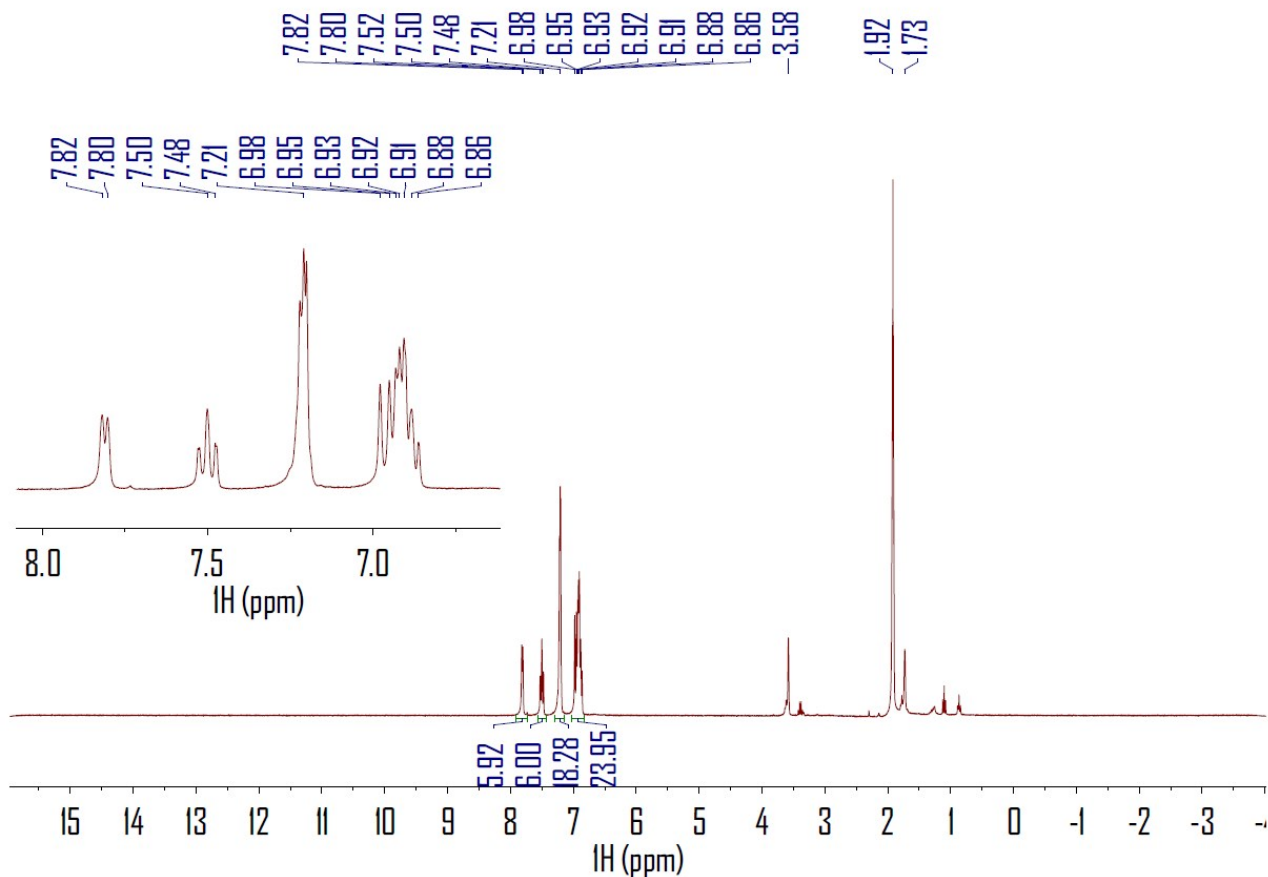


Figure S9. ^1H NMR spectrum of compound $(\text{L}^{\text{Ph}}\text{Sn})_3\text{PF}_6$ in $\text{THF-}d_8/\text{MeCN-}d_3$ (1:1).

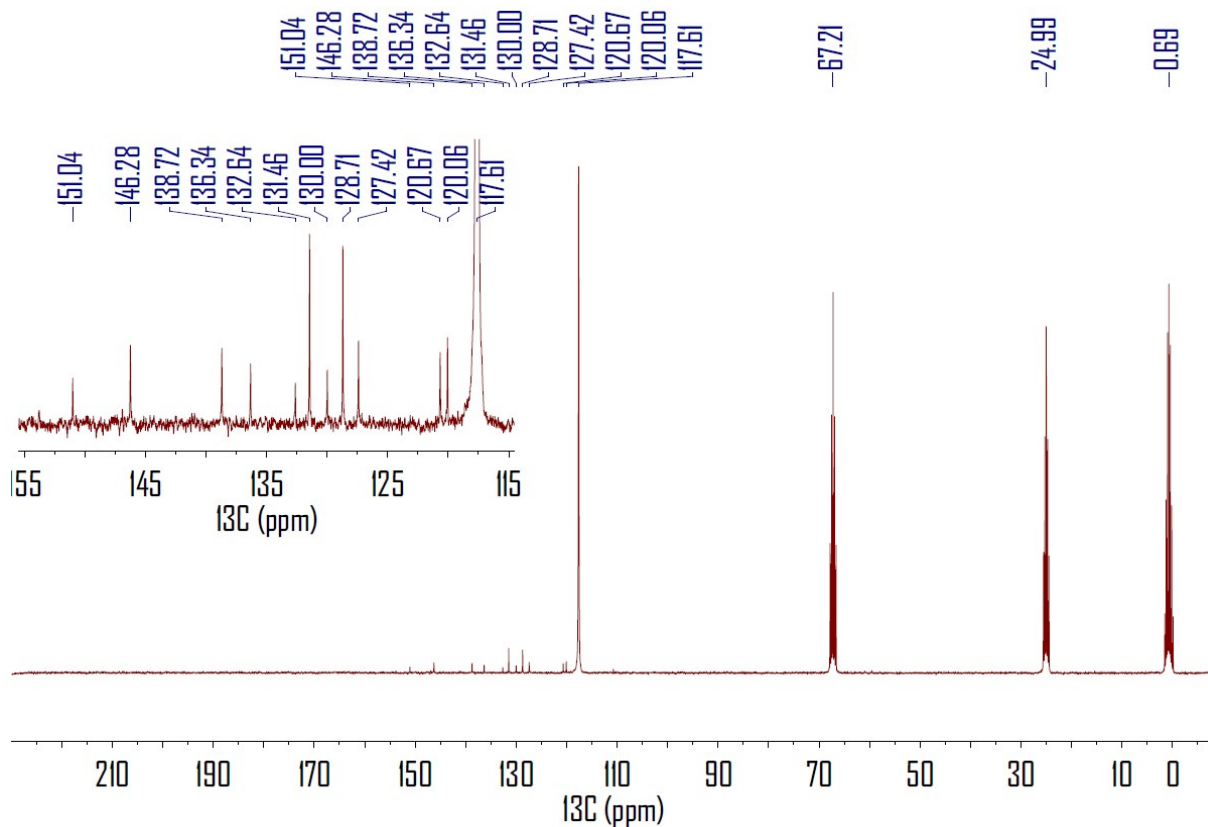
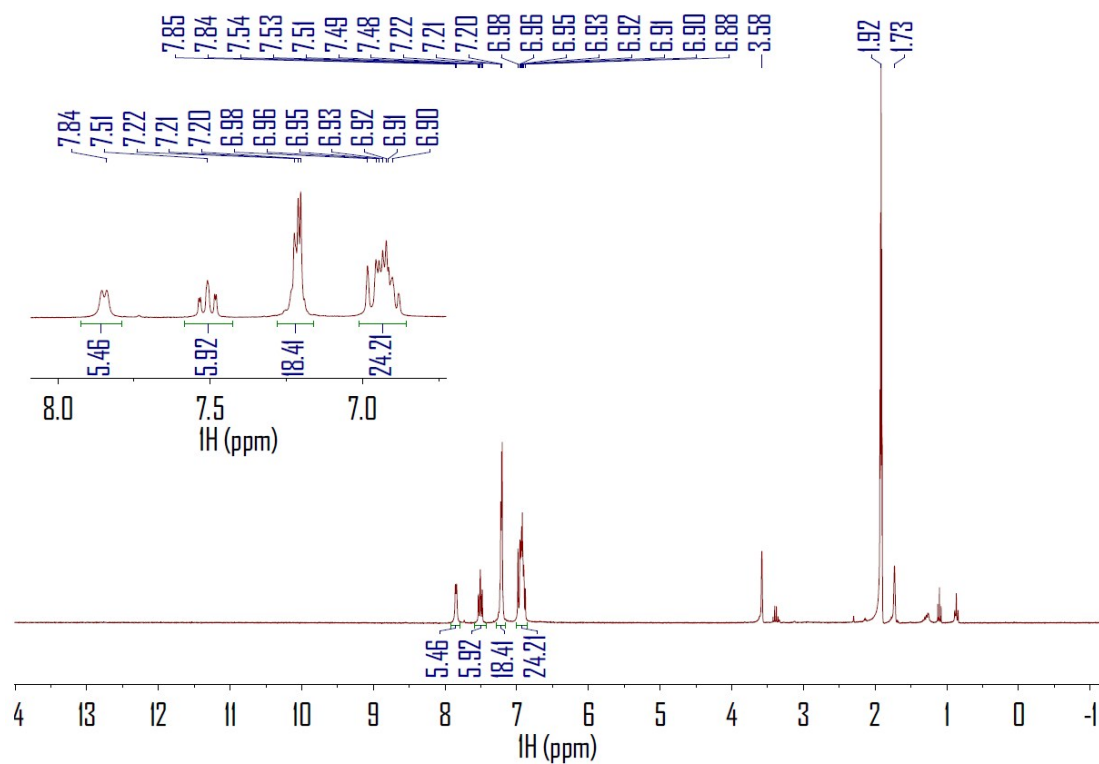
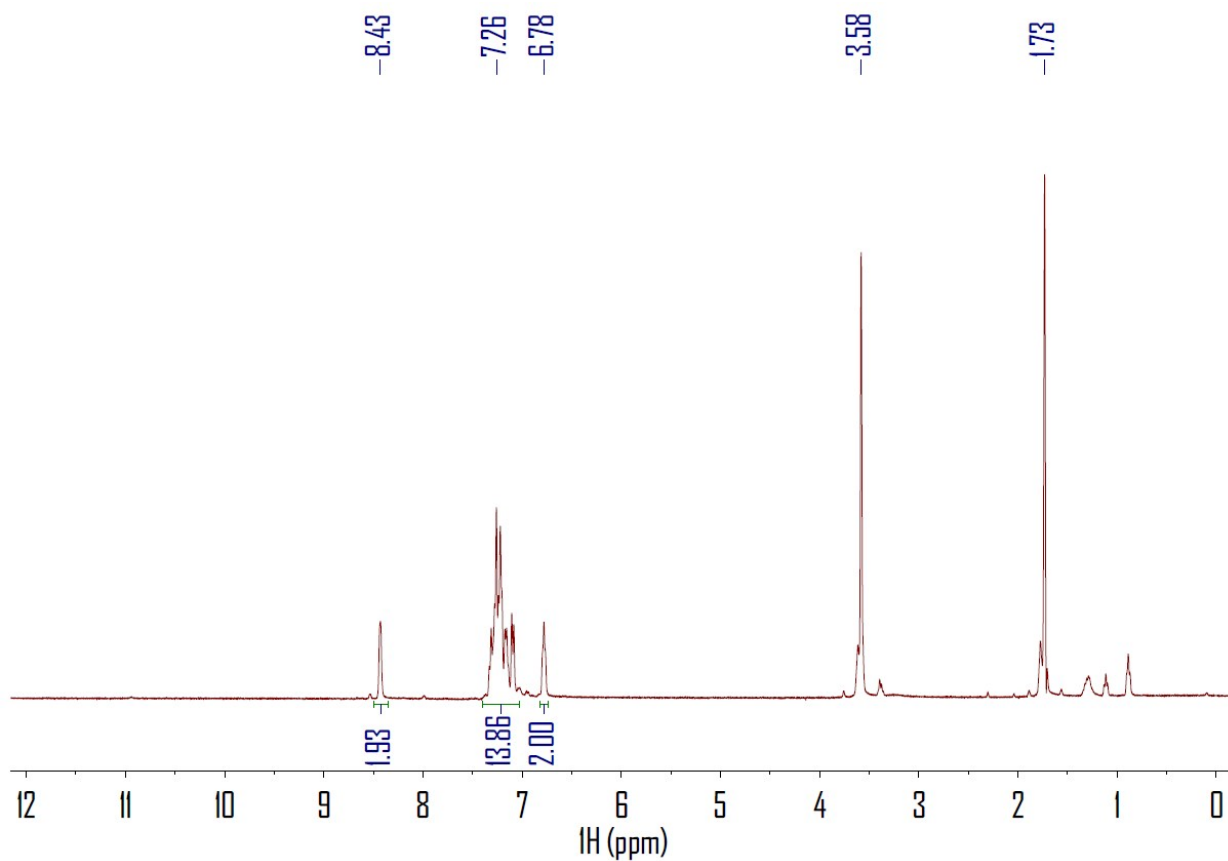


Figure S10. $^{13}\text{C}\{^1\text{H}\}$ NMR spectrum of compound $(\text{L}^{\text{Ph}}\text{Sn})_3\text{PF}_6$ in $\text{THF-}d_8/\text{MeCN-}d_3$ (1:1).



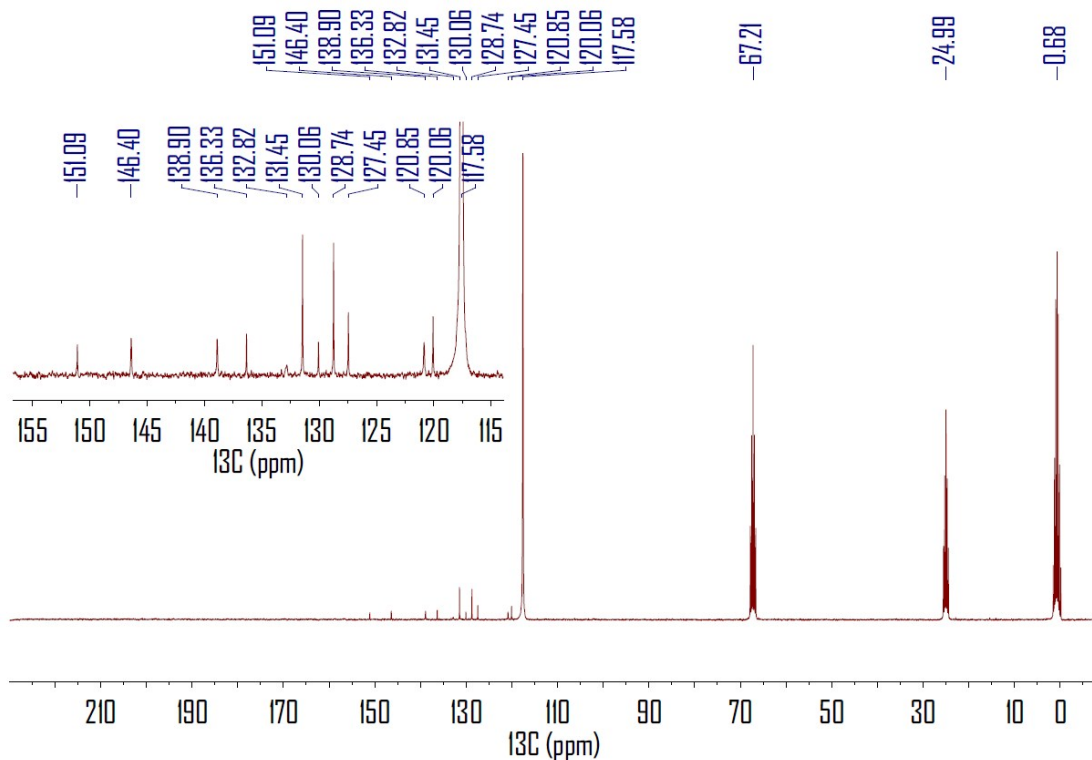


Figure S13. ^{13}C NMR spectrum of $(\text{L}^{\text{Ph}}\text{Sn})_3\text{AlCl}_4$ in $\text{THF-}d_8/\text{MeCN-}d_3$ (1:1).

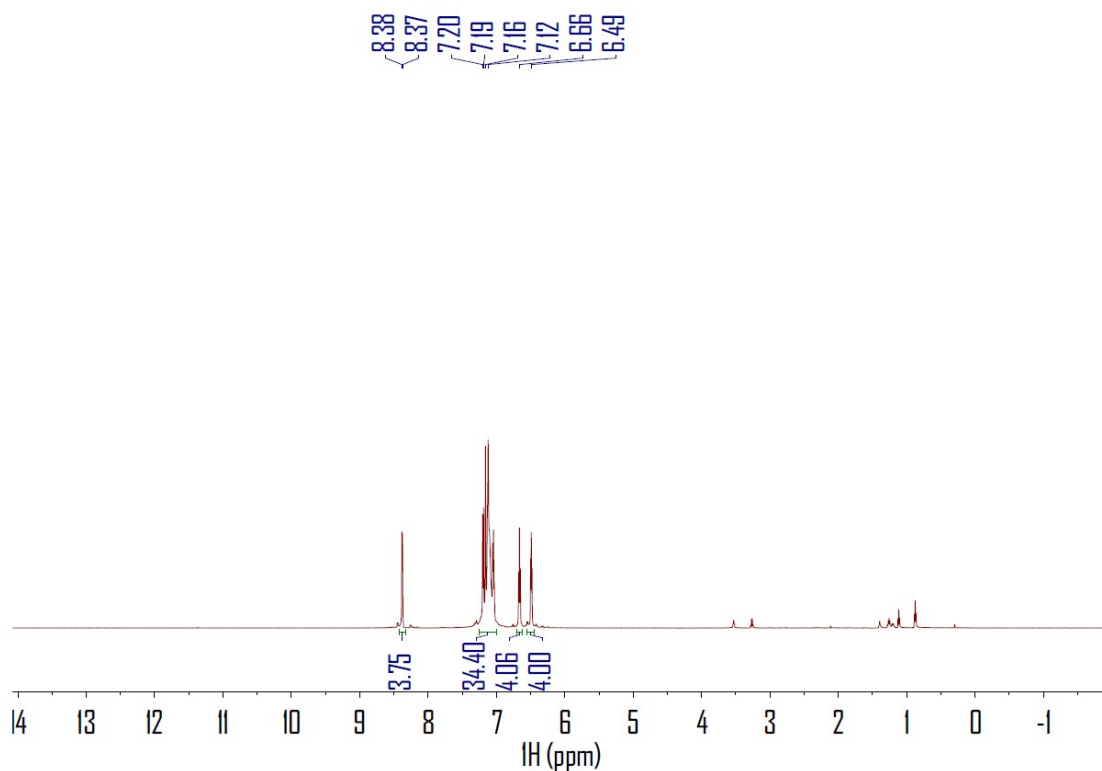


Figure S14. ^1H NMR spectrum of $(\text{L}^{\text{Ph}}\text{Sn})_2(\text{W}(\text{CO})_5)_2$ in C_6D_6 .

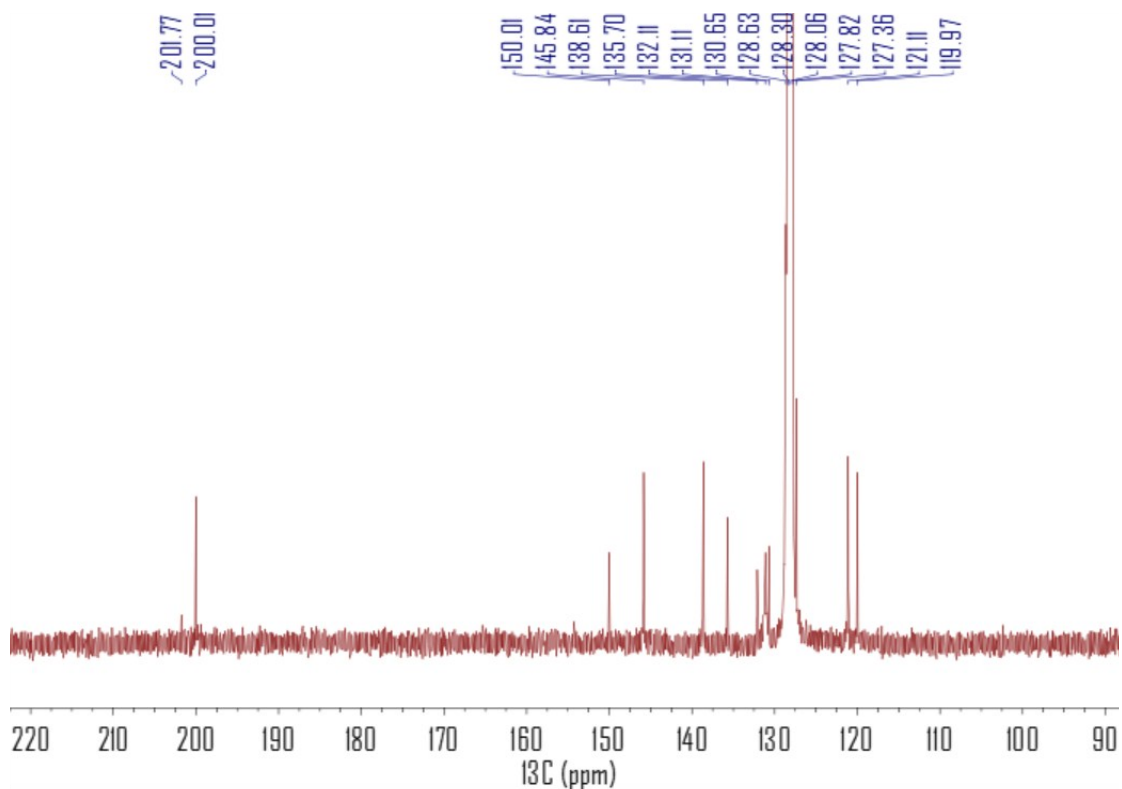


Figure S15. $^{13}\text{C}\{^1\text{H}\}$ NMR spectrum of $(\text{L}^{\text{PhSn}})_2(\text{W}(\text{CO})_5)_2$ in C_6D_6 .

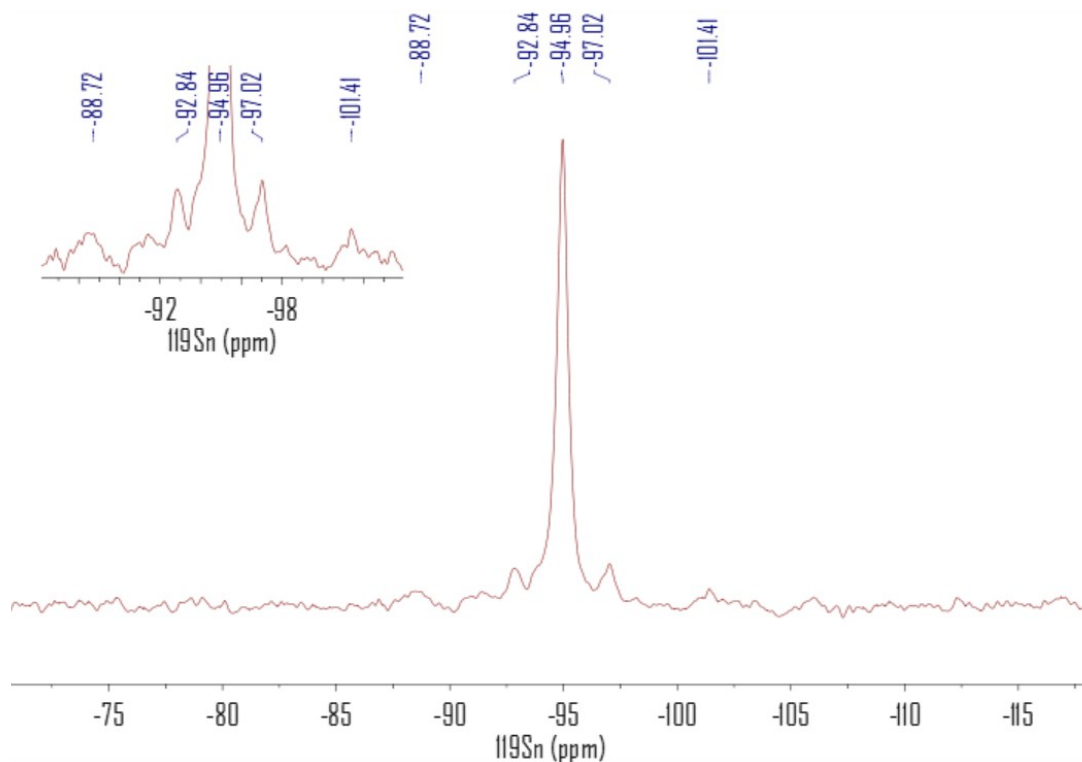


Figure S16. $^{119}\text{Sn}\{^1\text{H}\}$ NMR spectrum of $(\text{L}^{\text{PhSn}})_2(\text{W}(\text{CO})_5)_2$ in C_6D_6 .

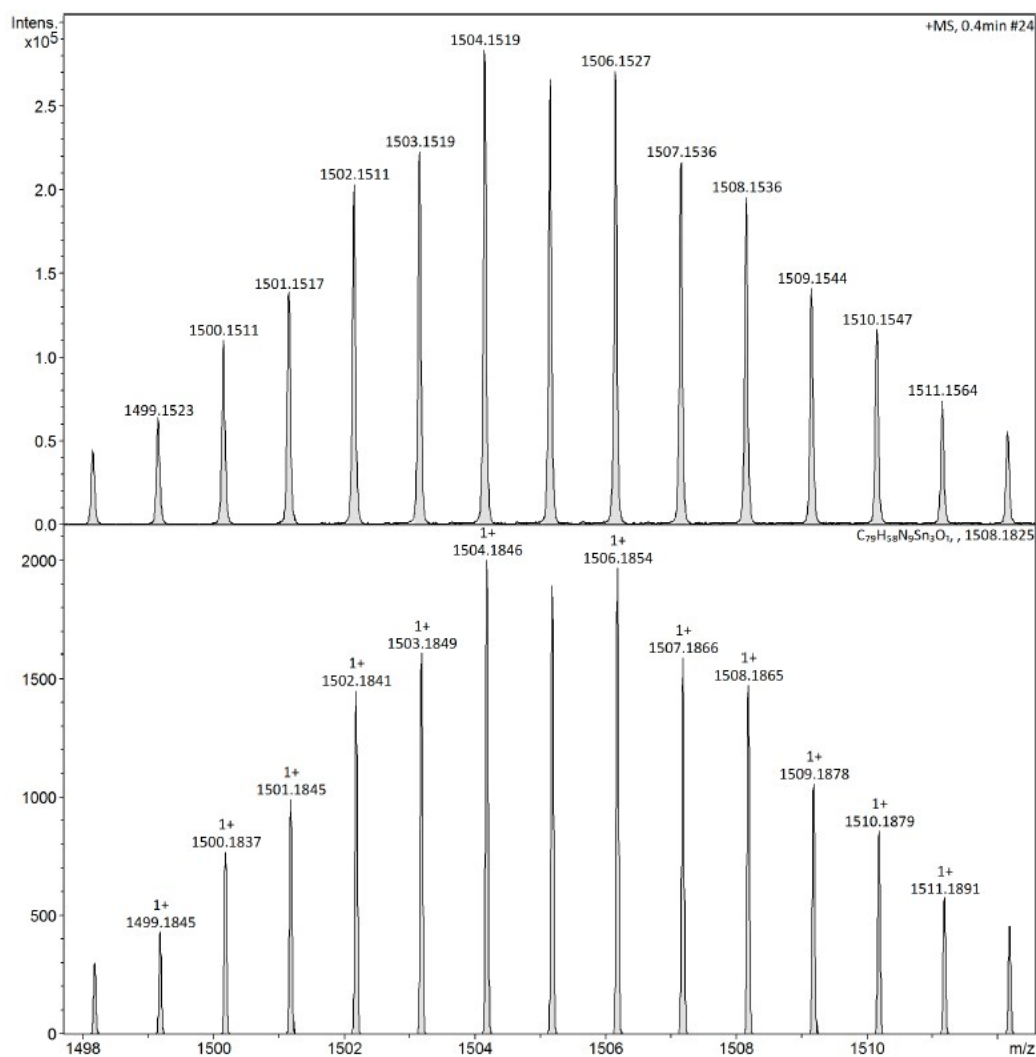


Figure S17. HR-ESIMS spectrum of $(L^{Ph})_3Sn_3OTf$ showing the molecular peak of $\{(L^{Ph})_3Sn_3MeOH\}^+$ (MeOH as eluent). Top: the experimental result; bottom: the simulation result.

2. Details on Raman measurement and data analysis

A laboratory constructed confocal Raman micro-spectrometer operating with a stabilized 532 nm laser (CW Nd:YVO₄; Verdi-V5, Coherent) was used for experiments (Fig. 1). The laser wavelength was stabilized using a high-resolution wavelength meter (WS-7, HighFinesse) along with a piezo-controller at 18789.995 (± 0.003) cm⁻¹. The excitation beam was directed into an inverted microscope (iX71, Olympus) after passing through a Faraday isolator, laser line filter and a linear polarizer (Glan Taylor prism). A long working distance objective (20 \times , NA 0.25, $f = 25$ mm, Olympus SLMPLN20x) was used to focus laser beam inside the sample. Laser power of around 2 mW for all the samples. Backscattered light collected using the same objective lens passed through a confocal setup consisting of a 100 μ m pinhole. After the confocal setup, Rayleigh scattering was removed using three Volume Bragg-notch filters (OptiGrate) allowing for low frequency Raman measurement down to 10 cm⁻¹ checked using L-cysteine. Collimated beam of Raman scattered photons were focused on the polychromator slit ($f=50$ cm, $f/6.5$, 600 gr/mm grating, SP-2500i, Princeton Instruments, slit width=100 μ m) using an achromatic cylindrical lens. Spectral resolution was determined to be ~ 3.5 cm⁻¹. The spectra were recorded using a Peltier cooled CCD (DU970N-BV, Andor) operating at -85°C.

Wavenumber calibration was performed using emission lines from neon and vacuum wavelength data from Atomic Spectra Database, NIST. Collected Raman spectra were reduced by multiplying $\tilde{\nu}_0^{-1}(\tilde{\nu}_0 - \tilde{\nu}_s)^{-3}[1 - \exp(-hc\tilde{\nu}/k_B T)]$, in order to remove the contribution of the Boltzmann population and the frequency factor to the Raman intensities.

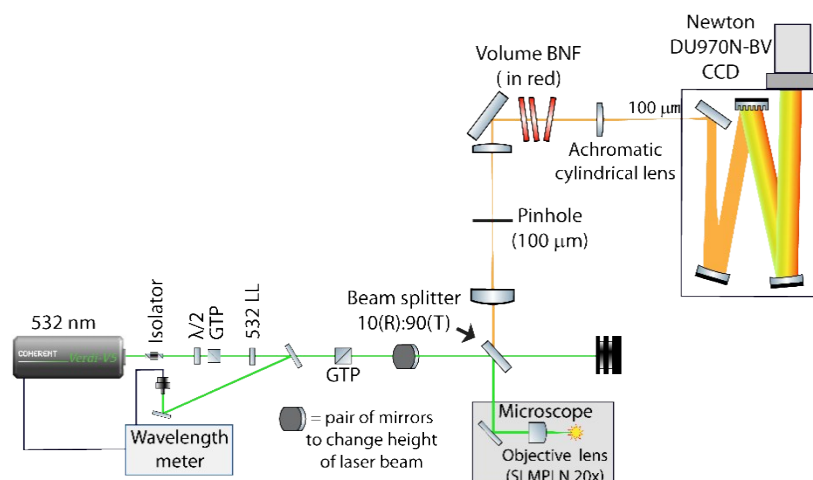


Figure S18. Optical setup of the Raman spectrometer used in the present work. In brief, a narrow band laser beam is directed in the microscope. Sample is placed on the microscope stage where it is exposed to the excitation laser. Back scattered Raman photons from the focal point are collected utilizing a confocal setup. Rayleigh scattering is rejected using narrow pass Bragg Notch Filters giving low wavenumber measurement capability. High sensitivity photon detection is performed using cooled CCD.

3. Single-crystal X-ray diffraction crystal structure figures and data tables

Single-crystal X-ray diffraction were performed on a Bruker APEX DUO diffractometer with APEX II 4K and multi-layer mirror monochromated Mo K α radiation ($\lambda = 0.71073 \text{ \AA}$) at 200(2) K. Data collection and reduction were performed with Bruker APEX II software. All of non-hydrogen atoms are refined anisotropically. Hydrogen atoms attached to the carbons were fixed at calculated positions and refined using a riding mode. Multiple disordered solvent molecules were observed in the crystal structures of all complexes. Whenever possible, co-crystallizing solvent molecules were modeled. Otherwise, SQUEEZE was employed to treat diffuse solvent contribution in the voids.

Table S1. Crystal data and structure refinement for **2(L^{Ph}SnCl) \cdot THF**

Empirical formula	C ₅₆ H ₄₄ Cl ₂ N ₆ OSn ₂	
Formula weight	1125.25	
Temperature	200(2) K	
Wavelength	0.71073 \AA	
Crystal system	Monoclinic	
Space group	P2 ₁ /c	
Unit cell dimensions	a = 24.7397(16) \AA	$\alpha = 90^\circ$
	b = 11.8214(8) \AA	$\beta = 105.783(2)^\circ$
	c = 17.2848(9) \AA	$\gamma = 90^\circ$
Volume	4864.5(5) \AA^3	
Z	4	
Density (calculated)	1.536 Mg/m ³	
Absorption coefficient	1.184 mm ⁻¹	
F(000)	2256	
Crystal size	0.42 x 0.33 x 0.04 mm ³	
Theta range for data collection	2.15 to 25.10 $^\circ$	
Index ranges	-29 \leq h \leq 29, -14 \leq k \leq 14, -19 \leq l \leq 20	
Reflections collected	111868	
Independent reflections	8607 [R(int) = 0.0499]	
Completeness to theta = 25.10 $^\circ$	99.5 %	
Absorption correction	multi-scan	
Max. and min. transmission	0.9542 and 0.6362	
Refinement method	Full-matrix least-squares on F ²	
Data / restraints / parameters	8607 / 0 / 604	
Goodness-of-fit on F ²	1.068	
Final R indices [$I > 2\sigma(I)$]	R1 = 0.0231, wR2 = 0.0467	
R indices (all data)	R1 = 0.0324, wR2 = 0.0510	
Largest diff. peak and hole	0.305 and -0.435 e/ \AA^3	

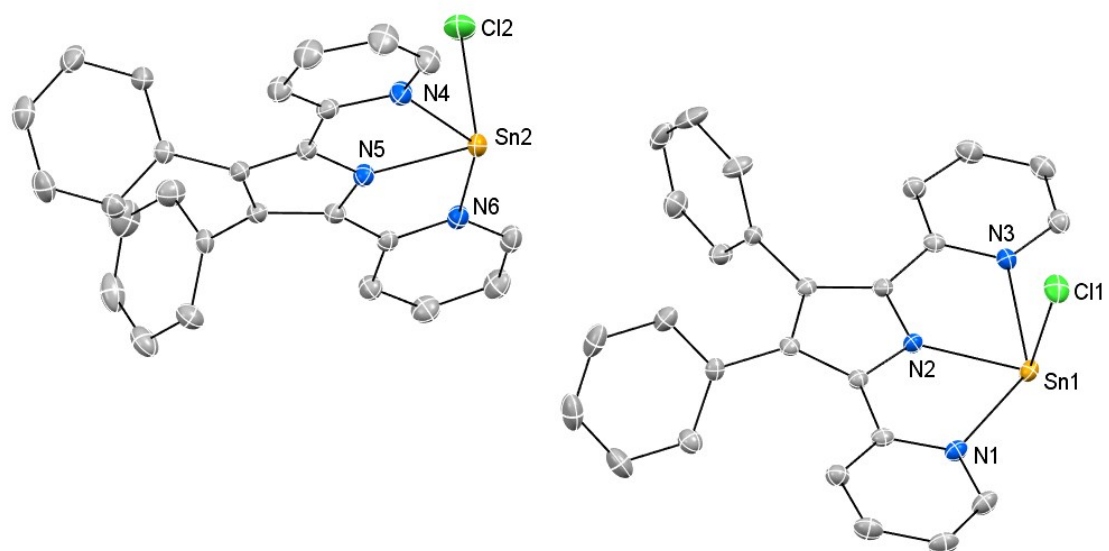


Figure S19. ORTEP diagram of $L^{\text{Ph}}\text{SnCl}$ (30% thermal ellipsoids; hydrogen atoms omitted). Selected interatomic distances (Å) and angles ($^{\circ}$): N(2)–Sn(1) 2.1489(18), Cl(1)–Sn(1) 2.4702(6), N(1)–Sn(1) 2.4724(19), N(3)–Sn(1) 2.4389(19), N(5)–Sn(2) 2.1476(19), Cl(2)–Sn(2) 2.4882(7), N(4)–Sn(2) 2.420(2), N(6)–Sn(2) 2.523(2); N(2)–Sn(1)–Cl(1) 93.69(5), N(5)–Sn(2)–Cl(2) 91.33(6).

Table S2. Crystal data and structure refinement for **(L^{Ph}Sn)₃Cl**

Empirical formula	C ₇₈ H ₅₄ ClN ₉ Sn ₃	
Formula weight	1508.82	
Temperature	200(2) K	
Wavelength	0.71073 Å	
Crystal system	Triclinic	
Space group	<i>P</i> -1	
Unit cell dimensions	a = 14.4606(16) Å	α = 94.697(2)°
	b = 15.1842(16) Å	β = 98.687(3)°
	c = 19.5168(18) Å	γ = 92.921(3)°
Volume	4213.2(8) Å ³	
Z	2	
Density (calculated)	1.189 Mg/m ³	
Absorption coefficient	0.955 mm ⁻¹	
F(000)	1504	
Crystal size	0.11 x 0.05 x 0.03 mm ³	
Theta range for data collection	2.12 to 25.07°	
Index ranges	-17 ≤ h ≤ 17, -18 ≤ k ≤ 18, -22 ≤ l ≤ 23	
Reflections collected	84778	
Independent reflections	14916 [R(int) = 0.0894]	
Completeness to theta = 25.07°	99.7 %	
Absorption correction	multi-scan	
Max. and min. transmission	0.9719 and 0.9022	
Refinement method	Full-matrix least-squares on F ²	
Data / restraints / parameters	14916 / 0 / 814	
Goodness-of-fit on F ²	0.881	
Final R indices [I > 2σ(I)]	R1 = 0.0492, wR2 = 0.1177	
R indices (all data)	R1 = 0.0928, wR2 = 0.1382	
Largest diff. peak and hole	1.088 and -0.935 e/Å ³	

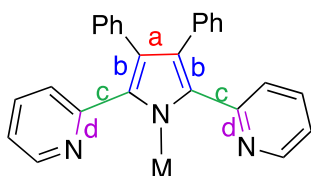


Table S2a. Comparison of selected bond lengths around pyrrole moieties in $(L^{Ph}Sn)_3Cl$ and $L^{Ph}H$

		in $(L^{Ph}Sn)_3Cl$	in $L^{Ph}H$ (free ligand)
a (Å)	top	1.419(6)	1.427(7)
	central	1.409(8)	
	bottom	1.418(8)	
b (Å)	top	1.406(6)	1.387(7)
	top	1.387(7)	
	central	1.416(7)	
	central	1.402(7)	
	bottom	1.422(8)	
	bottom	1.404(8)	
c (Å)	top	1.451(7)	1.467(7)
	top	1.467(6)	
	central	1.441(7)	
	central	1.442(7)	
	bottom	1.429(8)	
	bottom	1.491(8)	
d (Å)	top	1.360(6)	1.339(7)
	top	1.362(6)	
	central	1.363(6)	
	central	1.369(6)	
	bottom	1.351(8)	
	bottom	1.350(8)	

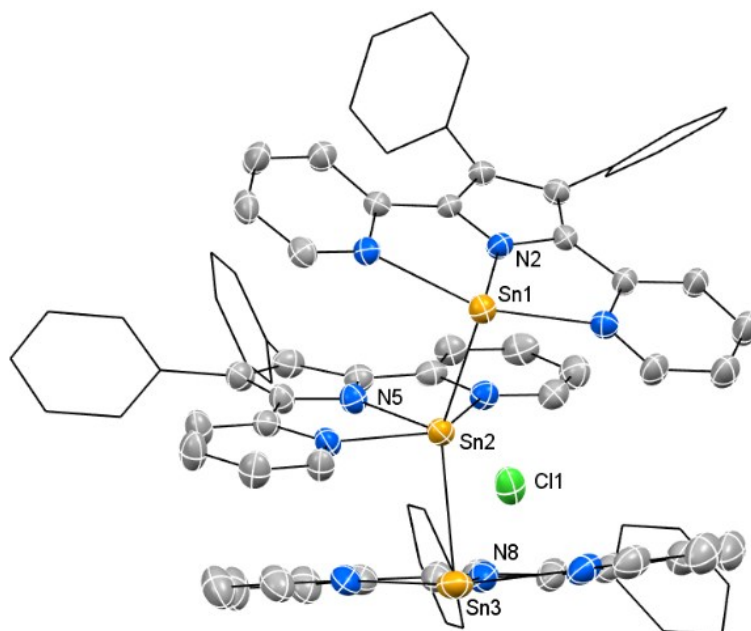


Figure S20. ORTEP diagram of $(L^{Ph}Sn)_3Cl$ (30% thermal ellipsoids; hydrogen atoms omitted). Selected interatomic distances (Å) and angles ($^\circ$): Sn(1)–Sn(2) 2.8521(6), Sn(2)–Sn(3) 2.8632(6), N(2)–Sn(1) 2.151(4), N(5)–Sn(2) 2.129(4), N(8)–Sn(3) 2.152(5), Cl(1)–Sn(1) 3.557(1), Cl(1)–Sn(2) 3.231(2), Cl(1)–Sn(3) 3.713(2); Sn(1)–Sn(2)–Sn(3) 145.070(16), N(2)–Sn(1)–Sn(2) 91.97(11), N(5)–Sn(2)–Sn(1) 106.50(12), N(5)–Sn(2)–Sn(3) 107.57(12), N(8)–Sn(3)–Sn(2) 92.50(12).

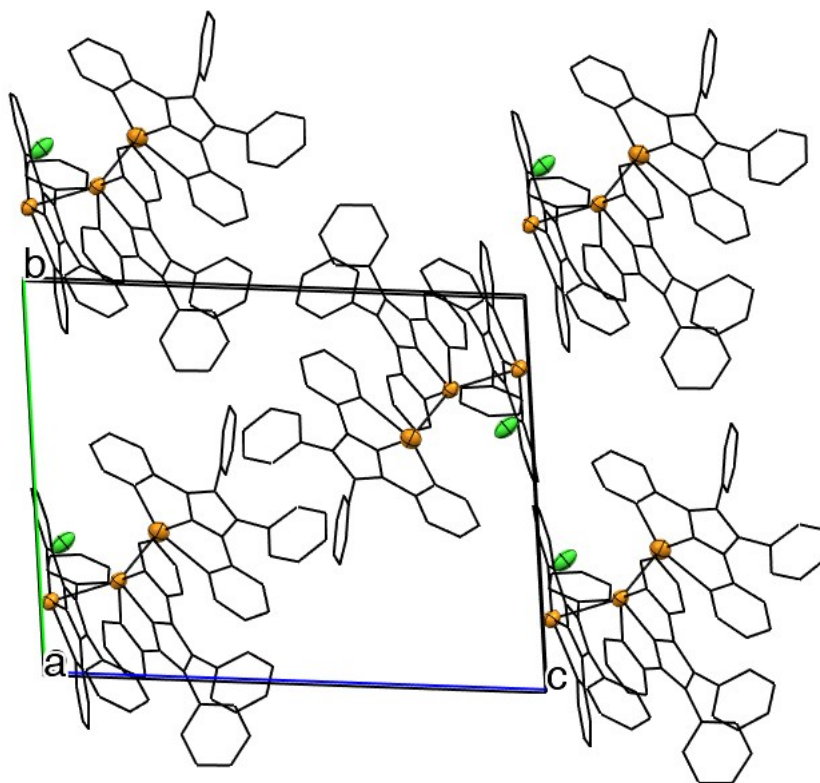


Figure S20a. Crystal packing diagram of $(L^{Ph}Sn)_3Cl$ (30% thermal ellipsoids; hydrogen atoms omitted).

Table S3. Crystal data and structure refinement for **(L^{Ph}Sn)₃OTf·2THF**

Empirical formula	C ₈₇ H ₇₀ F ₃ N ₉ O ₅ SSn ₃	
Formula weight	1766.65	
Temperature	200(2) K	
Wavelength	0.71073 Å	
Crystal system	Monoclinic	
Space group	<i>P</i> 2 ₁ / <i>c</i>	
Unit cell dimensions	<i>a</i> = 22.9751(7) Å	$\alpha = 90^\circ$
	<i>b</i> = 20.5456(7) Å	$\beta = 109.1750(10)^\circ$
	<i>c</i> = 17.8253(6) Å	$\gamma = 90^\circ$
Volume	7947.4(5) Å ³	
Z	4	
Density (calculated)	1.477 Mg/m ³	
Absorption coefficient	1.027 mm ⁻¹	
F(000)	3552	
Crystal size	0.38 x 0.36 x 0.22 mm ³	
Theta range for data collection	2.12 to 25.03°	
Index ranges	-26 ≤ <i>h</i> ≤ 27, -24 ≤ <i>k</i> ≤ 24, -21 ≤ <i>l</i> ≤ 21	
Reflections collected	74095	
Independent reflections	14014 [R(int) = 0.0426]	
Completeness to theta = 25.03°	99.6 %	
Absorption correction	multi-scan	
Max. and min. transmission	0.8056 and 0.6963	
Refinement method	Full-matrix least-squares on F ²	
Data / restraints / parameters	14014 / 0 / 971	
Goodness-of-fit on F ²	1.031	
Final R indices [<i>I</i> > 2σ(<i>I</i>)]	R1 = 0.0353, wR2 = 0.0783	
R indices (all data)	R1 = 0.0454, wR2 = 0.0827	
Largest diff. peak and hole	0.903 and -0.662 e/Å ³	

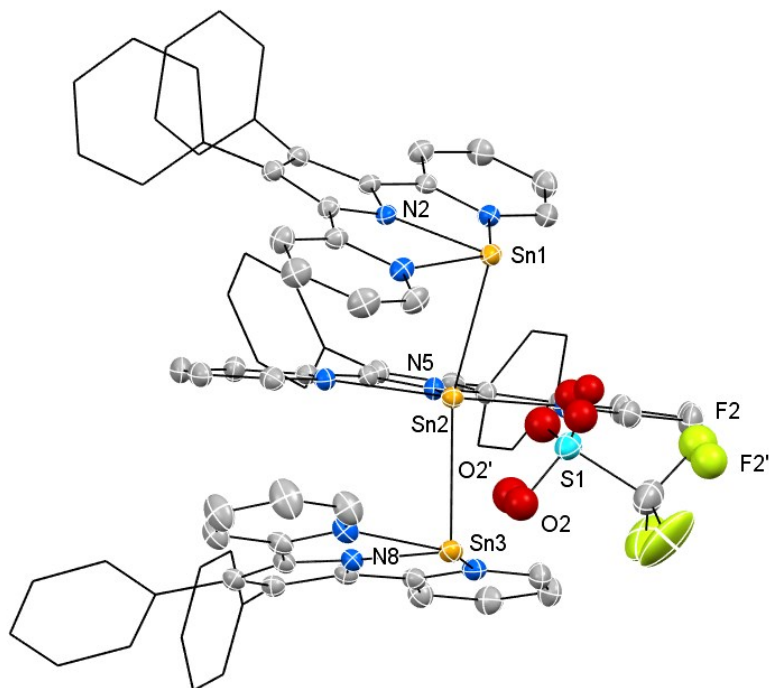


Figure S21. ORTEP diagram of $(L^{Ph}Sn)_3OTf$ (30% thermal ellipsoids; hydrogen atoms omitted). Selected interatomic distances (Å) and angles ($^{\circ}$): Sn(1)–Sn(2) 2.8922(3), Sn(2)–Sn(3) 2.9034(3), N(2)–Sn(1) 2.144(3), N(5)–Sn(2) 2.119(3), N(8)–Sn(3) 2.155(3); Sn(1)–Sn(2)–Sn(3) 145.658(11), N(2)–Sn(1)–Sn(2) 90.27(7), N(5)–Sn(2)–Sn(1) 107.40(7), N(5)–Sn(2)–Sn(3) 105.79(7), N(8)–Sn(3)–Sn(2) 88.52(7).

Table S4. Crystal data and structure refinement for **(L^{Ph}Sn)₃PF₆·Et₂O**

Empirical formula	C ₈₂ H ₆₄ F ₆ N ₉ OPSn ₃	
Formula weight	1692.46	
Temperature	200(2) K	
Wavelength	0.71073 Å	
Crystal system	Monoclinic	
Space group	<i>P</i> 2 ₁ / <i>c</i>	
Unit cell dimensions	<i>a</i> = 22.9606(18) Å	$\alpha = 90^\circ$
	<i>b</i> = 20.1323(15) Å	$\beta = 109.571(2)^\circ$
	<i>c</i> = 17.3947(14) Å	$\gamma = 90^\circ$
Volume	7576.2(10) Å ³	
Z	4	
Density (calculated)	1.484 Mg/m ³	
Absorption coefficient	1.069 mm ⁻¹	
F(000)	3384	
Crystal size	0.39 x 0.38 x 0.06 mm ³	
Theta range for data collection	2.14 to 25.06°	
Index ranges	-27 ≤ <i>h</i> ≤ 24, -23 ≤ <i>k</i> ≤ 23, -19 ≤ <i>l</i> ≤ 20	
Reflections collected	108419	
Independent reflections	13382 [R(int) = 0.0904]	
Completeness to theta = 25.06°	99.7 %	
Absorption correction	multi-scan	
Max. and min. transmission	0.9387 and 0.6806	
Refinement method	Full-matrix least-squares on F ²	
Data / restraints / parameters	13382 / 0 / 895	
Goodness-of-fit on F ²	1.079	
Final R indices [<i>I</i> > 2σ(<i>I</i>)]	R1 = 0.0776, wR2 = 0.2013	
R indices (all data)	R1 = 0.1123, wR2 = 0.2220	
Largest diff. peak and hole	2.208 and -1.595 e/Å ³	

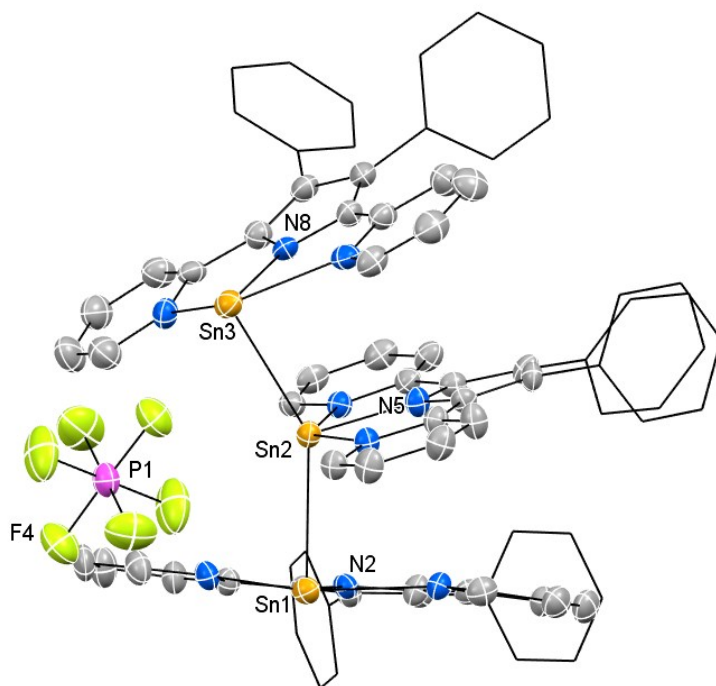


Figure S22. ORTEP diagram of $(L^{Ph}Sn)_3PF_6$ (30% thermal ellipsoids; hydrogen atoms omitted).

Selected interatomic distances (Å) and angles (°): Sn(1)–Sn(2) 2.8990(9), Sn(2)–Sn(3) 2.9149(9), N(2)–Sn(1) 2.131(6), N(5)–Sn(2) 2.108(6), N(8)–Sn(3) 2.156(7); Sn(1)–Sn(2)–Sn(3) 146.56(3), N(2)–Sn(1)–Sn(2) 91.72(17), N(5)–Sn(2)–Sn(1) 106.91(19), N(5)–Sn(2)–Sn(3) 105.63(19), N(8)–Sn(3)–Sn(2) 87.82(17).

Table S5. Crystal data and structure refinement for (L^{Ph})₂Sn

Empirical formula	C ₅₂ H ₃₆ N ₆ Sn	
Formula weight	863.56	
Temperature	200(2) K	
Wavelength	0.71073 Å	
Crystal system	Monoclinic	
Space group	C2/c	
Unit cell dimensions	a = 39.999(3) Å	α = 90°
	b = 13.8693(9) Å	β = 113.174(3)°
	c = 18.718(2) Å	γ = 90°
Volume	9546.4(14) Å ³	
Z	8	
Density (calculated)	1.202 Mg/m ³	
Absorption coefficient	0.574 mm ⁻¹	
F(000)	3520	
Crystal size	0.40 x 0.15 x 0.02 mm ³	
Theta range for data collection	2.18 to 25.07°	
Index ranges	-47<=h<=47, -16<=k<=16, -21<=l<=22	
Reflections collected	59437	
Independent reflections	8446 [R(int) = 0.0889]	
Completeness to theta = 25.07°	99.6 %	
Absorption correction	multi-scan	
Max. and min. transmission	0.9886 and 0.8029	
Refinement method	Full-matrix least-squares on F ²	
Data / restraints / parameters	8446 / 0 / 532	
Goodness-of-fit on F ²	0.926	
Final R indices [I>2sigma(I)]	R1 = 0.0457, wR2 = 0.1074	
R indices (all data)	R1 = 0.0767, wR2 = 0.1217	
Largest diff. peak and hole	0.468 and -0.649 e/Å ³	

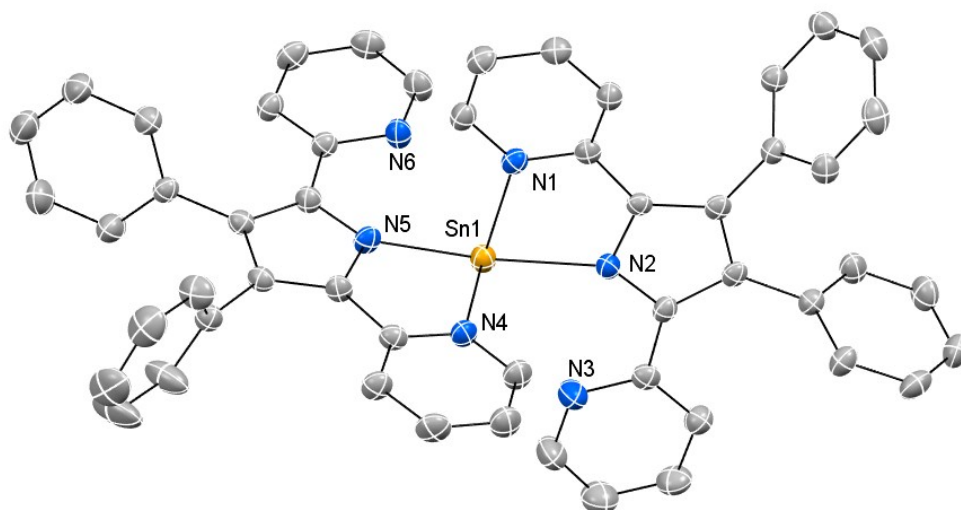


Figure S23 ORTEP diagram of $(L^{\text{Ph}})_2\text{Sn}$ (30% thermal ellipsoids; hydrogen atoms omitted). Selected interatomic distances (Å) and angles ($^\circ$): N(1)–Sn(1) 2.394(3), N(2)–Sn(1) 2.334(3), N(4)–Sn(1) 2.389(3), N(5)–Sn(1) 2.275(3), N(1)–Sn(1) 2.395(3), N(3)–Sn(1) 2.965(3), N(4)–Sn(1) 2.389(3), N(6)–Sn(1) 2.835(3); N(5)–Sn(1)–N(2) 139.94(11).

Table S6. Crystal data and structure refinement for $(\text{L}^{\text{Ph}}\text{Sn})_2(\text{W}(\text{CO})_5)_2$

Empirical formula	C ₆₂ H ₃₆ N ₆ O ₁₀ Sn ₂ W ₂	
Formula weight	1630.05	
Temperature	200(2) K	
Wavelength	0.71073 Å	
Crystal system	Triclinic	
Space group	P -1	
Unit cell dimensions	a = 11.0407(11) Å	$\alpha = 95.079(2)^\circ$
	b = 13.7762(12) Å	$\beta = 98.842(3)^\circ$
	c = 20.4412(19) Å	$\gamma = 111.909(3)^\circ$
Volume	2813.9(5) Å ³	
Z	2	
Density (calculated)	1.924 Mg/m ³	
Absorption coefficient	5.018 mm ⁻¹	
F(000)	1556	
Crystal size	0.15 x 0.13 x 0.08 mm ³	
Theta range for data collection	2.21 to 25.04°	
Index ranges	-13 ≤ h ≤ 13, -16 ≤ k ≤ 16, -24 ≤ l ≤ 24	
Reflections collected	87260	
Independent reflections	9911 [R(int) = 0.1126]	
Completeness to theta = 25.04°	99.5 %	
Absorption correction	multi-scan	
Max. and min. transmission	0.6896 and 0.5199	
Refinement method	Full-matrix least-squares on F ²	
Data / restraints / parameters	9911 / 0 / 739	
Goodness-of-fit on F ²	0.908	
Final R indices [I > 2σ(I)]	R1 = 0.0662, wR2 = 0.1539	
R indices (all data)	R1 = 0.1046, wR2 = 0.1760	
Largest diff. peak and hole	2.365 and -1.188 e/Å ³	

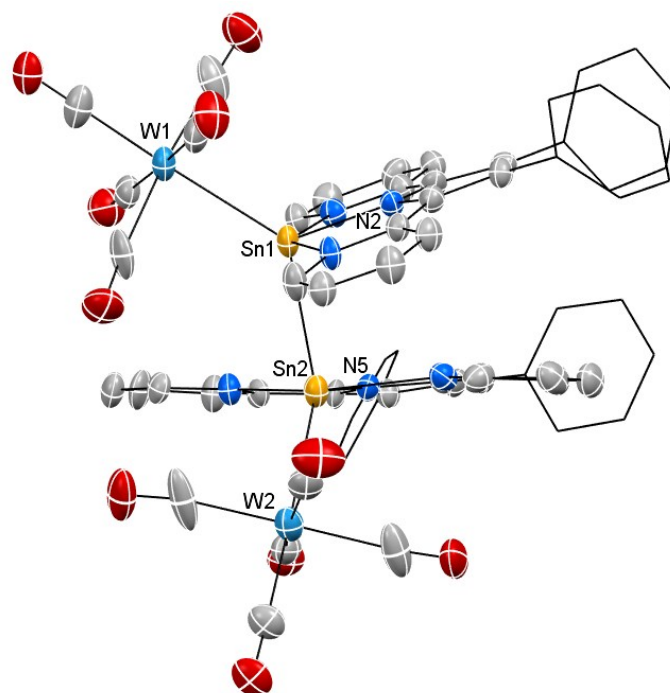


Figure S24. ORTEP diagram of $(L^{Ph}Sn)_2(W(CO)_5)_2$ (30% thermal ellipsoids; hydrogen atoms omitted). Selected interatomic distances (Å) and angles (°): Sn(1)–Sn(2) 2.9054(13), Sn(1)–W(1) 2.7618(10), Sn(2)–W(2) 2.7577(11), N(2)–Sn(1) 2.076(9), N(5)–Sn(2) 2.104(10); W(1)–Sn(1)–Sn(2) 133.15(4), W(2)–Sn(2)–Sn(1) 141.30(4), N(2)–Sn(1)–W(1) 126.9(3), N(2)–Sn(1)–Sn(2) 99.9(3), N(5)–Sn(2)–Sn(1) 101.8(3), N(5)–Sn(2)–W(2) 116.7(3).

4. Computational details

Density Functional Theory (DFT) was applied by the means of the M06-2X hybrid functional,^[3] corrected for dispersion as proposed by Grimme (D3 correction, BJ damping).^[4] Calculations were performed with the Gaussian 16 suite of programs.^[5] Geometry optimizations were performed without any symmetry constraints using the Def2-TZVP basis set^[6] for all atoms. NBO analyses were performed with NBO 6.0.^[6]

Table S7. Comparison of selected bond lengths and bond angles between solid state structure and calculated structure of **(L^{Ph}Sn)₃Cl**

	Experimental (crystal structure) data of (L^{Ph}Sn)₃Cl	Calculated structure of (L^{Ph}Sn)₃Cl
N _{pyrrole(2)} –Sn(1)	2.151(4) Å	2.200 Å
N _{pyrrole(5)} –Sn(2)	2.129(4) Å	2.188 Å
N _{pyrrole(8)} –Sn(3)	2.152(5) Å	2.199 Å
Sn(1)–Sn(2)	2.8521(6) Å	2.872 Å
Sn(2)–Sn(3)	2.8632(6) Å	2.890 Å
Cl(1)–Sn(1)	3.557(1) Å	3.509 Å
Cl(1)–Sn(2)	3.231(2) Å	3.059 Å
Cl(1)–Sn(3)	3.713(2) Å	3.560 Å
Sn(1)–Sn(2)–Sn(3)	145.070(16)°	143.895°
N _{pyrrole(2)} –Sn(1)–Sn(2)	91.97(11)°	88.000°
N _{pyrrole(5)} –Sn(2)–Sn(1)	106.50(12)°	105.626°
N _{pyrrole(5)} –Sn(2)–Sn(3)	107.57(12)°	110.270°
N _{pyrrole(8)} –Sn(3)–Sn(2)	92.50(12)°	92.514°

Coordinates for the optimized structure of **(L^{Ph}Sn)₃Cl**

C	4.11945	-1.91524	-2.18716
H	3.93957	-2.98468	-2.24796
C	5.3585	-1.41794	-1.83396
H	6.17363	-2.09181	-1.60977
C	5.51316	-0.03571	-1.78891
H	6.46921	0.40009	-1.52655
C	4.44367	0.78544	-2.0818
H	4.54994	1.85925	-2.06668
C	3.21534	0.20714	-2.42227
C	2.01119	0.94778	-2.77373
C	1.68778	2.31301	-2.84915
C	2.52131	3.47902	-2.5023
C	2.99784	3.64816	-1.20134
H	2.79406	2.87958	-0.46209
C	3.72359	4.77819	-0.85334
H	4.07223	4.89436	0.16476
C	3.98494	5.7577	-1.80326
H	4.5466	6.64218	-1.53179
C	3.52017	5.59716	-3.10154
H	3.7209	6.35534	-3.84762
C	2.79229	4.46779	-3.44731
H	2.41677	4.34785	-4.45617
C	0.35609	2.3824	-3.3144
C	-0.37584	3.62442	-3.61767
C	-0.39662	4.69077	-2.71607
H	0.13104	4.59252	-1.77583
C	-1.06451	5.86738	-3.02032
H	-1.06661	6.68201	-2.30718
C	-1.72242	6.00537	-4.23546
H	-2.24284	6.92401	-4.47299
C	-1.69428	4.96093	-5.14992
H	-2.18764	5.06426	-6.10799
C	-1.0206	3.78719	-4.84588
H	-0.98329	2.97976	-5.56802
C	-0.07586	1.04974	-3.46253
C	-1.3708	0.41603	-3.66692

C	-2.58678	1.09428	-3.81824
H	-2.60063	2.17283	-3.8504
C	-3.75865	0.3701	-3.87787
H	-4.70498	0.88611	-3.98118
C	-3.72259	-1.01892	-3.78641
H	-4.62204	-1.61483	-3.81715
C	-2.49184	-1.62846	-3.64232
H	-2.38937	-2.70576	-3.53994
C	-1.81413	0.74405	-0.61024
H	-2.49559	0.01481	-1.04214
C	-2.16042	2.08109	-0.51791
H	-3.12417	2.4193	-0.87161
C	-1.2255	2.95395	0.01766
H	-1.44861	4.01071	0.09379
C	-0.00302	2.47389	0.45743
H	0.7384	3.14284	0.87048
C	0.25846	1.10667	0.36545
C	1.47231	0.43733	0.83075
C	2.59642	0.8308	1.57844
C	2.86984	2.1223	2.2346
C	1.94311	2.69427	3.10896
H	0.99638	2.19186	3.27009
C	2.2291	3.87511	3.7784
H	1.49917	4.29694	4.45778
C	3.45471	4.50236	3.59436
H	3.68294	5.41879	4.12264
C	4.38676	3.94156	2.7316
H	5.34602	4.42155	2.58294
C	4.09543	2.76588	2.05527
H	4.82345	2.33013	1.38024
C	3.44367	-0.30173	1.64944
C	4.71538	-0.34974	2.39674
C	5.90907	-0.73946	1.78844
H	5.89088	-1.03016	0.7455
C	7.10134	-0.75418	2.49821
H	8.0162	-1.05981	2.00623
C	7.12478	-0.36743	3.83134
H	8.05452	-0.37426	4.38501
C	5.94688	0.03543	4.44639
H	5.95559	0.34658	5.48316
C	4.75612	0.04527	3.73584
H	3.84066	0.37667	4.21139
C	2.77628	-1.33141	0.96256
C	3.00524	-2.75708	0.76905
C	4.10566	-3.47001	1.25504
H	4.86265	-2.96203	1.83198
C	4.20068	-4.8237	0.99793
H	5.04883	-5.38288	1.3724
C	3.20619	-5.46186	0.26505
H	3.25044	-6.51811	0.04335
C	2.12918	-4.70925	-0.16414
H	1.30231	-5.13999	-0.72209
C	0.86219	-2.25579	3.43216
H	1.26788	-3.18789	3.04962
C	1.55837	-1.49935	4.3552
H	2.53538	-1.81374	4.69433
C	0.95457	-0.33881	4.82439
H	1.45136	0.27772	5.56367
C	-0.28658	0.03359	4.34424
H	-0.77607	0.92411	4.70872
C	-0.90379	-0.75656	3.37037
C	-2.17575	-0.45787	2.7229
C	-3.10086	0.59387	2.82363

C	-3.04393	1.80874	3.6604
C	-2.01976	2.74284	3.50256
H	-1.248	2.54935	2.76779
C	-1.992	3.90558	4.25874
H	-1.19241	4.62144	4.11343
C	-2.99622	4.15776	5.18459
H	-2.97973	5.06594	5.77293
C	-4.02467	3.23926	5.34591
H	-4.81324	3.42918	6.06262
C	-4.0492	2.07648	4.58929
H	-4.85655	1.3646	4.70983
C	-4.16601	0.26986	1.95404
C	-5.37633	1.09237	1.77209
C	-5.27198	2.44327	1.43687
H	-4.28741	2.87404	1.29873
C	-6.40565	3.23048	1.29759
H	-6.30414	4.27619	1.03681
C	-7.66569	2.68249	1.49617
H	-8.55023	3.2967	1.38906
C	-7.78308	1.34344	1.84551
H	-8.76046	0.91126	2.01856
C	-6.6481	0.55895	1.9883
H	-6.73802	-0.48219	2.27613
C	-3.81698	-0.94626	1.34243
C	-4.38724	-1.7458	0.26687
C	-5.57209	-1.44643	-0.4144
H	-6.12332	-0.55188	-0.1696
C	-6.02227	-2.31147	-1.39138
H	-6.94501	-2.09536	-1.91591
C	-5.28792	-3.45116	-1.69832
H	-5.6114	-4.15216	-2.45456
C	-4.1021	-3.66387	-1.02043
H	-3.45559	-4.50495	-1.24434
N	3.08423	-1.13215	-2.47469
N	0.94177	0.21619	-3.15369
N	-1.35488	-0.9306	-3.58896
N	-0.64418	0.27765	-0.19514
N	1.60412	-0.85912	0.48635
N	2.03209	-3.4009	0.0867
N	-0.32629	-1.89973	2.95652
N	-2.62908	-1.36736	1.83247
N	-3.66444	-2.83326	-0.07254
Sn	0.84752	-1.97378	-3.33562
Sn	0.11391	-2.07208	-0.56054
Sn	-1.69359	-3.29416	1.33526
Cl	-0.95028	-4.61548	-1.88629

5. References

- [1] A. McSkimming, V. Diachenko, R. London, K. Olrich, C. J. Onie, M. M. Bhadbhade, M. P. Bucknall, R. W. Read, S. B. Colbran, *Chem. Eur. J.* **2014**, *20*, 11445-11456.
- [2] a) D. H. Harris, M. F. Lappert, *J. Chem. Soc., Chem. Commun.* **1974**, 895-896; b) C. D. Schaeffer, L. K. Myers, S. M. Coley, J. C. Otter, C. H. Yoder, *J. Chem. Educ.* **1990**, *67*, 347.
- [3] Y. Zhao, D. G. Truhlar, *The Journal of Chemical Physics* **2006**, *125*, 194101.
- [4] a) S. Grimme, J. Antony, S. Ehrlich, H. Krieg, *The Journal of Chemical Physics* **2010**, *132*, 154104; b) S. Grimme, S. Ehrlich, L. Goerigk, *J. Comput. Chem.* **2011**, *32*, 1456-1465.
- [5] M. J. Frisch, G. W. Trucks, H. B. Schlegel, G. E. Scuseria, M. A. Robb, J. R. Cheeseman, G. Scalmani, V. Barone, G. A. Petersson, H. Nakatsuji, X. Li, M. Caricato, A. V. Marenich, J. Bloino, B. G. Janesko, R. Gomperts, B. Mennucci, H. P. Hratchian, J. V. Ortiz, A. F. Izmaylov, J. L. Sonnenberg, Williams, F. Ding, F. Lipparini, F. Egidi, J. Goings, B. Peng, A. Petrone, T. Henderson, D. Ranasinghe, V. G. Zakrzewski, J. Gao, N. Rega, G. Zheng, W. Liang, M. Hada, M. Ehara, K. Toyota, R. Fukuda, J. Hasegawa, M. Ishida, T. Nakajima, Y. Honda, O. Kitao, H. Nakai, T. Vreven, K. Throssell, J. A. Montgomery Jr., J. E. Peralta, F. Ogliaro, M. J. Bearpark, J. J. Heyd, E. N. Brothers, K. N. Kudin, V. N. Staroverov, T. A. Keith, R. Kobayashi, J. Normand, K. Raghavachari, A. P. Rendell, J. C. Burant, S. S. Iyengar, J. Tomasi, M. Cossi, J. M. Millam, M. Klene, C. Adamo, R. Cammi, J. W. Ochterski, R. L. Martin, K. Morokuma, O. Farkas, J. B. Foresman, D. J. Fox, Wallingford, CT, **2016**.
- [6] F. Weigend, R. Ahlrichs, *Physical Chemistry Chemical Physics* **2005**, *7*, 3297-3305.